UNIVERSITY OF LATVIA
Faculty of Physics and Mathematics

RAIMONDS VIĻUMS

Conservative Averaging Method in Mathematical Models of Heat Processes of Electric Systems

Ph.D. Thesis

Scientific supervisor
Prof., Dr. Habil. Math.
ANDRIS BUIĶIS

ISBN 978-9934-8180-1-1

RĪGA, 2010

Abstract

In the PhD thesis, original mathematical models are developed using and generalizing the conservative averaging method to study heat flux in electric wires, automotive fuses and electro-welding, which is a new process of joining wires. In statements, quasi-linear differential equations are used, and non-linearity of physical parameters is taken into account. Implemented in software, the models are solvable in a short time interval and easily adaptable for new materials and changes in the dimensions of the object. The theoretical basis of conservative averaging is generalized for a polar/cylindrical coordinate system and supplemented with exponential approximation. All the tasks are related to topical problems of industry and come from major German companies. The research has been carried out together with Munich Bundeswehr University.

Keywords

conservative averaging, mathematical model, fuse, wire, electro-welding

Table of Contents

Introduction

The contents of this Ph.D. thesis reflect the collaboration of the University of Latvia's Faculty of Physics and Mathematics and a science group based at the Munich Bundeswehr University's Department of Electrical Engineering and Information Technology (*Universität der Bundeswehr München, Fakultät für Elektrotechnik und Informationstechnik*), led by Prof. Dr. Ing. Hans-Dieter Liess (*Ließ*).

In the Ph.D. thesis, original mathematical models are developed for various electrical systems, which describe how they heat up under the influence of current, thermal conductivity and other physical processes. The problems being studied are primarily related to vehicle-safety issues, e.g., stability of fuses and estimation of the thermal endurance of wire insulation. In the mathematical models, quasi-linear differential equations are used, and the non-linearity of physical parameters is taken into account in describing such processes as heat convection with the surrounding environment or surface heat radiation.

The **first** chapter contains a general overview of the conservative averaging method, which is used for the formation of all the models considered in the Ph.D. thesis. Using this method, it's possible to reduce the full three-dimensional problem with complex geometry to a simpler mathematical model which is easier to use in practice.

The conservative averaging method was developed in the 1980's by A. Buikis for partial differential equations with discontinuous coefficients, when he was modelling processes in environments with a layered structure [1]-[3]. There are various mathematical models of physical processes which use the method, made mostly by A. Buikis together with co-authors, e.g., cooling fin systems: [4]-[6]; plywood production [7]; convective diffusion process in aquifer for oil pumping [8]; and steel quenching: [9], [10]. The conservative averaging is also used to construct several types of the integral splines for heat or filtration processes in general multi-layer domains (e.g. [11]-[14]).

Originally, the method was created for the Cartesian coordinate system, using polynomial approximation. In his Master's thesis [15], the author already presented the general form of the approximation by exponential functions (such type of approximation was used only for several particular models before, e.g. [4]). In order to use additionally the method in a polar or cylindrical coordinate system, inferences were made in the Ph.D. thesis using both polynomial and exponential approximation.

The necessity to use the polar coordinate system arose during the first joint assignment realised together with the Bundeswehr University and Vilnius Technical University, in which the safety of electrical wire insulation in vehicles (trams, trolleybuses) was studied within the framework of the Eureka Project.

The **second** chapter considers a mathematical model that makes it possible to calculate the distribution of time-dependent temperature within the wire and its insulation. Similar problems have been numerically solved with the finite element method throughout the whole domain before, e.g. [16], [17]. In this thesis, the properties of that sub-domain that characterise the electrical conductor (metal) with the conservative averaging method are transferred to the inner side of the insulation as a non-classical boundary condition. As a result, it is only necessary to do numerical calculations in the insulation sub-domain – afterwards, the temperature in the metal is restored analytically.

The task to research electrical fuses arose during the continuation of the collaboration with Bundeswehr University of Munich, which in turn collaborates with German car manufacturers. The essence of the problem is that the functioning and overheating of fuses does not always occur as expected and tested in technological laboratories, e.g., after a slight electrical overload, fuses tend to break faster than specified in the standards. The goal of the study was, firstly, to model and understand how current car fuses heat up, and secondly, to formulate recommendations for the elimination of shortcomings and for the development of new fuses. Models known to the author and previously studied in literature were one-dimensional and utilised the chain principle, where the element is replaced with a range of thermal resistors, capacitors and heat sources: [18], [19].

The **third** chapter documents the development of a three-dimensional mathematical model for the fuse within the Cartesian coordinate system. Since the formulation of the problem is too complex to calculate many variations, the conservative averaging method is used to transform the mathematical model into a more easily usable form. From the initial three-dimensional system, mathematical models are obtained, which are based on a one-dimensional system of partial differential equations (time and single space dimension), as well as models that only contain the time-dependent ordinary differential equation system. The numerical results that were obtained from these mathematical models are mutually compared. The Ph.D. thesis demonstrates the use of the conservative averaging system for domains of a more complex form, not just for layered systems.

Calculating the developed models, it turned out that a significant quantity of heat from the fuse flows further into the electrical system if the strength of the electric current is near or slightly above the nominal value of the fuse. To model this situation, mathematical models were developed in which the flow of heat from the fuse to the wires attached to it was also taken into consideration. Geometry consisting of bodies of cylindrical form was admitted to be suitable, and, therefore, the cylindrical coordinate system was used. The mathematical models obtained are considered in the **fourth** chapter of the Ph.D. thesis. As before, they are based on quasi-linear three-dimensional or one-dimensional partial differential equations or ordinary differential equations. Numerical results from the varying models are compared among each other. Publication that reflected this research won an award of the best student paper in the 3rd WSEAS int. conference on Applied and Theoretical Mechanics in 2007 ([20], [21]).

In the **fifth** and final chapter of the Ph.D. thesis, the first mathematical models are developed for a new industrial process, which is called electro-welding. The ends of two electrical wires consisting of various metals are connected and subjected to a strong current, while they heat up and melt together. Since various metals were used, e.g., aluminium and brass, the task is to find out how long the free end of each wire should be to begin melting in the place where the connection occurs, rather than on the inside of the metal. At the time of writing the Ph.D. thesis, the numerical results obtained have been sent to a company that develops this technological process.

Collaboration with our foreign partners is due to continue in the future, improving the existing mathematical models and developing new ones. The main results of the Ph.D. thesis have been published in scientific journals and conference proceedings. The style of the text and sub-chapter structure has been retained as in the publications.

Together with co-authors, the author has 5 publications on the subject of the Ph.D. thesis. The author has reported on 6 international and 5 local conferences.

Importance of the Subject

Development of all the mathematical models referred in the Ph.D. thesis is related to problems which are currently topical in the industry. Industrial companies that think about the future and innovations collaborate with scientists and search for ways to improve existing technologies and implement new ones.

Studies of automotive fuses and electrical wires are conducted to increase the safety of vehicle electrical systems, as well as to reduce production costs; for example, needlessly oversized cables are often attached to electrical devices. Finding out what is a sufficient wire diameter would make it possible to save resources. In turn, in fuses, problems such as their overheating and degradation of an insulation of attached wire, which is not permissible from a safety perspective, have been observed.

In designing new vehicles, development of electrical systems requires even greater precision. Cars with hybrid engines and light emitting diode (LED) lamps encountered problems that were not relevant for vehicles of former generations.

Today, when introducing new materials and technologies, numerical calculations are important not only before their introduction in production, but already at the sample construction stage. For a new polymer insulation material whose physical properties are non-linearly dependent on temperature, heat flow modelling makes it possible to find appropriate dimensions of an electrical conductor that will not pose a threat to safety. Calculations for an electro-welding task, which is a new electrical wire connection method, reduce the number of practical experiments and save power resources.

Even though general modelling software of physical processes exists, development of a single specific model using such computer programs often requires too much time. In contrast, use of an effective and quickly calculated mathematical model makes it possible to reach the desired result faster.

The Objective of the Thesis

The objective of this Ph.D. thesis is to develop original and practical mathematical models using the conservative averaging method to study the thermal processes in electrical system elements, as well as to make calculations with real physical property values. The tasks to be carried out arise from formulated, practical problems in vehicle equipment and electro-welding.

Research Methodology

At first, the theoretical basis of the conservative averaging method is studied, generalizing it for polar/cylindrical coordinate system, as well as supplementing the method with exponential approximation. Researching particular problem, a three-dimensional mathematical model of the object and its physical properties is created. Using the conservative averaging method, the initial task is reduced to an ordinary or partial differential equation system with a reduced number of dimensions. Numerical results are compared among the mathematical models developed and experimental measurements.

Scientific Novelty and the Main Results

- The conservative averaging method for the polar/cylindrical coordinate system has been developed.
- The conservative averaging method has been supplemented with exponential approximation in both Cartesian and polar/cylindrical coordinate systems.
- An analytical transformation of the mathematical model of insulated electrical wire to a new problem, which contain only insulation domain, has been carried out. Finding its solution, temperature in conductor could be obtained analytically.
- An analytical reduction of the three-dimensional mathematical model of the automotive fuse to a one-dimensional mathematical problem (time and single space dimension) has been carried out, as well as a reduction to an ordinary differential equation system, which is solely time-dependent. Cylindrical and Cartesian (parallelepiped) geometries have been studied.
- Numerical results from various developed mathematical models have been mutually compared. The results of numerical calculations correspond to the experimental observations of real objects and confirm the adequacy of the developed mathematical models.
- The first mathematical models for electro-welding have been developed. Similar as before, the formulation of a three-dimensional problem has been transformed into several mathematical models with a smaller number of dimensions.
- The optimal lengths of the free ends of two metal wires have been discovered, which ensures maximum temperature during welding at the place where the connection occurs.

• The mathematical models developed can be numerically solved in a short time interval. Implemented in computer software, they can be easily adapted for new materials and changes in the dimensions of the object.

• To reduce the initial number of dimensions of the mathematical models, the conservative averaging method is used in all instances. The methodology studied in the Ph.D. thesis can also be used to develop other more complex mathematical models of thermal systems.

Applications

The developed mathematical models have helped to provide a better understanding of physical processes in the problems studied. Results of calculations are used to forecast the properties of real car fuses and electrical wires, as well as in developing the technological process of electro-welding. Conservative averaging made it possible to create such mathematical models whose numerical solution does not require much time, thus making it possible to calculate many examples quickly, which is not insignificant when collaborating with companies.

The techniques containing conservative averaging, which have been developed to obtain mathematical models in this thesis, make it possible to create models for other physical processes related to heat flows and electric current in a similar manner. In fact, the general overview of the conservative averaging method makes it possible to use the method for any problem involving second-order partial differential equations.

Acknowledgements

The research was supported by European Social Fund (ESF), University of Latvia, Council of Sciences of Latvia, Institute of Mathematics and Computer Science, and Munich Bundeswehr University.

Special thanks for a help to accomplish Ph.D. studies are expressed to scientific supervisor Prof. A. Buikis, Prof. Dr. Ing. H.-D. Liess, author's family and friends.

Publications, Reports on Conferences and International Cooperation

Publications

1. *Cylindrical Model of Transient Heat Conduction in Automotive Fuse Using Conservative Averaging Method.* **Viļums R., Liess H.-D., Buikis A. and Rudevičs A.** Athens : WSEAS Press, 2008. Proceedings of the 13rd WSEAS Int. Conf. on Applied and Computational Mathematics. Puerto De La Cruz, Tenerife, Spain, December 15 – 17, 2008. pp. 355-360. ISBN: 978-960-474-034-5.

2. *Conservative Averaging and Finite Difference Methods for Transient Heat Conduction in 3D Fuse.* **Viļums R. and Buikis A.** Athens : WSEAS Press, 2008, WSEAS Transactions on Heat and Mass Transfer, Vol. 3, Issue 1, pp. 111-124.

3. *Transient Heat Conduction in 3D Fuse Modeled by Conservative Averaging Method.* **Viļums R. and Buikis A.** Athens : WSEAS Press, 2007. Proceedings of the 3rd WSEAS Int. Conf. on Applied and Theoretical Mechanics (Mechanics '07). Puerto De La Cruz, Spain, December 14 – 16, 2007. pp. 54-59. Best student paper of the conference.

4. *Conservative Averaging Method for Partial Differential Equations with Discontinuous Coefficients.* **Viļums R. and Buikis A.** Athens : WSEAS Press, 2006, WSEAS Transactions on Heat and Mass Transfer, Vol. 1, Issue 4, pp. 383-390. ISSN: 1790-5044.

5. *Conservative Averaging Method and its Application for One Heat Conduction Problem.* **Viļums R. and Buikis A.** Athens : WSEAS Press, 2006. Proceedings of the 4th WSEAS Int. Conf. on Heat Transfer, Thermal Engineering and Environment. Elounda, Greece, August 21 – 23, 2006. pp. 226-231.

Reports on International Scientific Conferences

1. *Quasi-Linear Mathematical Model of Electro-Welding Process for Wires.* **Viļums R., Buikis A. and Liess H.-D.** Abstracts of the 13th Int. Conf. on Mathematical Modelling and Analysis (MMA) and 3rd Int. Conf. on Approximation Methods and Orthogonal Expansions, June 4 – 7, 2008, Kaariku, Estonia. Estonian Mathematical Society. p. 18.

2. *Transient Heat Conduction in 3D Fuse Modeled by Conservative Averaging Method.* **Viļums R. and Buikis A.** 3rd WSEAS Int. Conf. on Applied and Theoretical Mechanics (Mechanics '07). Puerto De La Cruz, Spain, December 14 – 16, 2007. Best student paper of the conference.

3. *Conservative Averaging Method for 2D Heat Transfer Problem in Multi-Cylinder System.* **Buikis A. and Viļums R.** Abstracts of the 12th Int. Conf. of Mathematical Modelling and Analysis (MMA), May 30 – June 2, 2007, Trakai, Lithuania. VGTU Press "Technika", 2007, Vilnius. p. 24.

4. *Quasi-One-Dimensional Mathematical Models for Car's Electrical Elements with Fuses.* **Viļums R., Liess H.-D., Ilgevicius A. and Buikis A.** Abstracts of the 12th Int. Conf. of Mathematical Modelling and Analysis (MMA), May 30 – June 2, 2007, Trakai, Lithuania. VGTU Press "Technika", 2007, Vilnius. p. 106.

5. *Conservative Averaging Method and its Application for One Heat Conduction Problem.* **Viļums R. and Buikis A.** 4rd WSEAS Int. Conf. on Heat Transfer, Thermal Engineering and Environment. Elounda, Greece, August 21-23, 2006.

6. *Analytically-Numerical Approach for the Heat Transfer in Wire with Insulation.* **Viļums R.** Abstracts of the 11th Int. Conf. of Mathematical Modelling and Analysis (MMA), May 31 – June 3, 2006, Jurmala, Latvia. p. 68.

7. *Conservative Averaging Method for Calculation of Heat Transfer in Cylindrical Wire with Insulation.* **Buikis A., Liess H.-D. and Viļums R.** Abstracts of the 10th Int. Conf. of Mathematical Modelling and Analysis (MMA), June 1 – 5, 2005, Trakai, Lithuania. Institute of Mathematics and Computer Science, Vilnius, 2005. p. 149.

Reports on Local Scientific Conferences

1. *Comparison of Multi-Dimensional Mathematical Models of Automotive Fuses.* **Viļums R.** 68th LU conference, Section of Mathematical Modelling and Numerical Analysis, Rīga, 25.02.2010.

2. *Integral exponential spline.* **Viļums R.** 65th LU conference, Section of New Scientists, Rīga, 08.02.2007.

3. *Calculation of the Heat Transfer in Cylindrical Wire with Insulation by Combination of Analytical and Numerical Methods.* **Viļums R.** 6th Latvian Mathematical Conference. Liepāja, April 7-8, 2006. Abstracts. LPA LiePA, Liepāja, 2006. p. 53.

4. *Conservative Averaging Method for Calculation of Heat Flow in Wire with Insulation.* **Viļums R.** 64th LU conference, Section of New Scientists, Rīga, 14.02.2006.

5. *Conservative Averaging Method for Two-Layer System in Polar Coordinates.* **Viļums R. and Buikis A.** 63rd LU conference, Section of Mathematical Modelling, Rīga, 10.02.2005.

International Cooperation

The research was carried out in collaboration with Prof. Dr. Ing. H.-D. Liess and his co-workers from Munich Bundeswehr University. During his studies, author visited the university 3 times: 1) October 22 – November 7, 2007; 2) October 9 – 31, 2008; 3) October 8 – November 9, 2009.

1 Conservative Averaging Method

The conservative averaging method was developed as approximate analytical and numerical method for solving partial differential equations with piecewise continuous coefficients: [1]-[3]. The usage of this method for a separate relatively thin sub-domain or for a sub-domain with a large heat conduction coefficient leads to the reduction of the domain in which the solution must be found. The method can be applied for several sub-domains simultaneously. To apply this method for all sub-domains of the layered media, a special type of spline is constructed: the integral averaged values interpolating spline. Usage of this spline allows diminishing dimensions of the initial problem one by one. There are other sources containing information about the conservative averaging method and its applications, e.g., [15], [22]-[25].

1.1 Main Concept

Built on a concrete steady-state heat conduction example, the main idea of the method is given in this section.

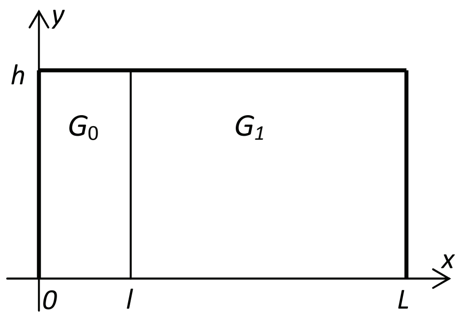

Fig. 1.1: Visualization of the domain

Let us assume that we have domain D that consists of two sub-domains (rectangles) G_0 and G_1 (Fig. 1.1):

$$G_0 = \{(x,y) \mid x \in (0,l), y \in (0,h)\},$$

$$G_1 = \{(x,y) \mid x \in (l,L), y \in (0,h)\},$$

$$D = G_0 \cup G_1 \cup \{(x,y) \mid x = l, y \in (0,h)\}.$$

The objective is to find function $U_0(x,y)$ (continuous in domain $\overline{G}_0$) and function $U_1(x,y)$ (continuous in domain $\overline{G}_1$) that fulfils the following equations:

a) heat transfer differential equations:

$$\frac{\partial}{\partial x}\left(k_0 \frac{\partial U_0}{\partial x}\right) + \frac{\partial}{\partial y}\left(k_0 \frac{\partial U_0}{\partial y}\right) + F_0(x,y) = 0, \tag{1}$$

$$\frac{\partial}{\partial x}\left(k_1 \frac{\partial U_1}{\partial x}\right) + \frac{\partial}{\partial y}\left(k_1 \frac{\partial U_1}{\partial y}\right) + F_1(x,y) = 0; \tag{2}$$

b) conjugation conditions at $x = l$ (i.e. continuity of temperature and heat flux):

$$U_0\big|_{x=l} = U_1\big|_{x=l}, \tag{3}$$

$$k_0 \frac{\partial U_0}{\partial x}\bigg|_{x=l-0} = k_1 \frac{\partial U_1}{\partial x}\bigg|_{x=l+0}; \tag{4}$$

c) boundary conditions:

$$\frac{\partial U_0}{\partial x}\bigg|_{x=0} = 0, \tag{5}$$

$$\frac{\partial U_1}{\partial x}\bigg|_{x=L} = 0, \tag{6}$$

$$\frac{\partial U_i}{\partial y}\bigg|_{y=0} = 0, \quad i = \overline{0,1}, \tag{7}$$

$$\left[k_i \frac{\partial U_i}{\partial y} - \alpha_i \left(U_i - \Theta \right) \right]\bigg|_{y=h} = 0. \tag{8}$$

We require that all derivatives of the equations (1) and (2) are continuous in corresponding sub-domains. The solution of this mathematical problem can be treated as temperature in two layer media for heat transfer process. Coefficient k is heat conductivity, and α is heat convection to the environment then. We assume that all coefficients are constant here. Temperature dependent coefficients are considered in the next chapters where conservative averaging is applied to specific models.

Let us assume that domain G_0 is thin in x-direction or it is made from material that has relatively better heat conductivity than the other one (or both conditions take place). We can obviously assume that temperature is almost constant in x-direction then. If this assumption was not reasonable, we could assume that distribution of the temperature differs from some other curve only slightly, i.e., polynomial or function of the exponential behaviour. Therefore, the first thing is to understand in which domain and in which direction the behaviour of the unknown function is predictable.

Before we choose a specific representative (i.e. approximation) function, we introduce integral averaged value function over chosen interval. If we take domain G_0 and interval $x \in [0, l]$, the definition of this function is

$$u_0(y) = \frac{1}{l} \int_0^l U_0(x, y) dx. \tag{9}$$

In our case, function u_0 represents averaged temperature in interval $x \in [0, l]$ on given line y.

Next, we select a function that will approximate our unknown function in chosen domain and segment. It should describe a particular physical situation. This means that the better view of the situation we have, the more appropriate function we can choose. For example, let us use exponential approximation in x-direction. Then, general form of the function U_0 is

$$U_0(x, y) = a(y) + b(y)\,\mathrm{e}^{x} + c(y)\,\mathrm{e}^{-x}. \tag{10}$$

The representation of the function U_0 contains unknown functions $a(y)$, $b(y)$, $c(y)$. These are obtained in such a way that they fulfil conditions on the boundaries $x = 0$ and $x = l$, and integral equality (9).

Practically, hyperbolic functions could be used instead of exponent:

$$U_0(x,y) = \tilde{a}(y) + \tilde{b}(y)\left(\cosh\left(\frac{x}{l}\right) - \sinh(1)\right) + \tilde{c}(y)\left(\sinh\left(\frac{x}{l}\right) - \cosh(1) + 1\right). \quad (11)$$

Taking into account derivative of this function:

$$\frac{\partial U_0}{\partial x} = \frac{1}{l}\tilde{b}(y)\sinh\left(\frac{x}{l}\right) + \frac{1}{l}\tilde{c}(y)\cosh\left(\frac{x}{l}\right); \quad (12)$$

and boundary condition on the border $x = 0$ (5), we obtain that $\tilde{c}(y) \equiv 0$. If we apply integral (9) to the approximation formula (11), we obtain that

$$\tilde{a}(y) = u_0(y).$$

Conjugation condition (4) on the boundary $x = l$ of the domain G_0 gives unknown function $\tilde{b}(y)$:

$$\tilde{b}(y) = \frac{lk_1}{\sinh(1)} \left.\frac{\partial U_1}{\partial x}\right|_{x=l}.$$

After unknown functions are found, we can rewrite approximation of the function U_0:

$$U_0(x,y) = u_0(y) + \frac{lk_1}{\sinh(1)}\left(\cosh\left(\frac{x}{l}\right) - \sinh(1)\right)\left.\frac{\partial U_1}{\partial x}\right|_{x=l}. \quad (13)$$

The next step of the conservative averaging method is integration of the main differential equation (1) over the interval $x \in [0,l]$:

$$\frac{1}{l}\int_0^l \left[\frac{\partial}{\partial x}\left(k_0 \frac{\partial U_0}{\partial x}\right) + \frac{\partial}{\partial y}\left(k_0 \frac{\partial U_0}{\partial y}\right) + F_0(x,y)\right] dx = 0.$$

Let us take a look at the first addend:

$$\frac{1}{l}\int_0^l \frac{\partial}{\partial x}\left(k_0 \frac{\partial U_0}{\partial x}\right) dx = \frac{k_0}{l}\left.\frac{\partial U_0}{\partial x}\right|_{x=l} - \frac{k_0}{l}\left.\frac{\partial U_0}{\partial x}\right|_{x=0} = \frac{k_1}{l}\left.\frac{\partial U_1}{\partial x}\right|_{x=l} - 0.$$

We used conditions (4) and (5) on the borders of the domain G_0 to make analytical transformations here. On the other hand, we could use representation (13) and it also would lead to the same result.

Order of the integration and derivation could be swapped for the other derivatives in the integral because of the assumption of continuity of the solution. After that, integral formula (9) is applied:

$$\frac{1}{l}\int_0^l \frac{\partial}{\partial y}\left(k_0 \frac{\partial U_0}{\partial y}\right) dx = \frac{\partial}{\partial y} k_0 \frac{\partial}{\partial y}\frac{1}{l}\int_0^l U_0 dx = \frac{d}{dy}\left(k_0 \frac{du_0}{dy}\right).$$

Consequently, differential equation for the unknown averaged value function $u_0(y)$ is the following:

$$\frac{d}{dy}\left(k_0 \frac{du_0}{dy}\right) + \frac{k_1}{l}\left.\frac{\partial U_1}{\partial x}\right|_{x=l} + f(y) = 0; \quad (14)$$

where $f(y)$ is averaged value of the source function:

$$f(y) := \frac{1}{l}\int_0^l F_0(x,y)dx .$$

We have transformed initial problem to the new one. Differential equation (2) for the function $U_1(x,y)$ in the domain G_1 remains the same. The second differential equation (14) is for the averaged value function $u_0(y)$ in interval $y \in [0,h]$.

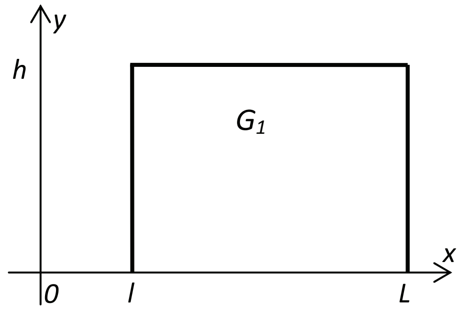

Fig. 1.2: Domain after conservative averaging

If we take into account representation of the averaged function (13), the conjugation condition (3) gives condition between functions u_0 and U_1:

$$u_0 = U_1\big|_{x=l} + lk_1\left(1-\tanh(1)\right)\frac{\partial U_1}{\partial x}\bigg|_{x=l} . \tag{15}$$

This equation together with the equation (14) could be considered as non-classical boundary condition for the border $x = l$ in domain G_1.

Boundary conditions when $y = 0$ and $y = h$ for the function u_0 are similar as for the function U_0:

$$\frac{du_0}{dy}\bigg|_{y=0} = 0 , \tag{16}$$

$$\left(k_0\frac{du_0}{dy} + h_y\left(u_0 - \Theta\right)\right)\bigg|_{y=h} = 0 . \tag{17}$$

To be accurate, these equalities are obtained after integral is applied to boundary conditions (7), (8). Transformations are similar to those that were done for the main differential equation (1). Boundary conditions (6)-(8) remain the same for the function $U_1(x,y)$ of the domain G_1.

We have transformed original problem and reduced dimensions of the domain (Fig. 1.2). Usually, it is impossible to find analytical solution of mathematical problem – the only choice is to solve it numerically. It takes less computer power to calculate such mathematical model because of reduced dimensions.

It is possible to reconstruct temperature distribution $U_0(x,y)$ in domain G_0 from the representation (13) after functions $u_0(y)$ and $U_1(x,y)$ are calculated. Note that it is possible to get value at any point of averaged interval – not only in some discrete points as it would be after applying finite difference method to initial problem.

Mathematical problem is reduced by one dimension for whole system if conservative averaging method is applied for the domain G_1 in x-direction over interval $x \in [l, L]$. Averaging procedure can be applied continuously in several directions, reducing dimensions of the problem one by one. Numerical calculations are also reduced by order.

Let us look back to the original problem (1)-(8). For both domains, conservative averaging could be applied in y-direction at first (Fig. 1.3).

Fig. 1.3: Domain after reduction of one dimension

Boundary conditions at $y = 0$ and $y = h$ transfer to the new differential equations then. If constant approximation in y-direction is used:

$$U_0(x, y) = u_0(y), \quad U_1(x, y) = u_1(y),$$

following differential equations are obtained:

$$\frac{d}{dx}\left(k_i \frac{du_i}{dx}\right) - \frac{\alpha_i}{h}(u_i - \Theta) = -f_i, \qquad f_i(x) = F_i(x, y), \quad i = \overline{0,1}. \tag{18}$$

Remaining boundary and conjugation conditions actually stay the same:

$$\left.\frac{du_0}{dx}\right|_{x=0} = 0, \quad \left.\frac{du_1}{dx}\right|_{x=L} = 0, \tag{19}$$

$$u_0\big|_{x=l} = u_1\big|_{x=l}, \quad k_0 \left.\frac{du_0}{dx}\right|_{x=l-0} = k_1 \left.\frac{du_1}{dx}\right|_{x=l+0}. \tag{20}$$

In conclusion, main steps of the conservative averaging method are summarized. First, choose function of the approximation. Second, integrate main differential equation. Third, use boundary and conjugation conditions.

1.2 Description of Conservative Averaging Method for Rectangular Two-Layer Domain in Cartesian Coordinate System

1.2.1 Original Problem with Neumann Boundary Condition

More general description of the method is given in this section. We start with statement of the problem again.

Let us look at domain D where

$$(x, y) \in D \subset R^{n+1}, \ x \in R, \ y = (y_1, \ldots, y_n) \in R^n.$$

Domain D consists of several sub-domains (for simplicity, we can imagine it as (n+1)-dimensional parallelepiped, see Fig. 1.4):

$$D = G_0 \cup G \cup H, \quad G_0 \cap G \cap H = \varnothing,$$

$$G_0 = \{(x, y) \mid x \in (-\delta, 0), y \in D\}, \quad G = \{(x, y) \mid x > 0, y \in D\}.$$

By notation $x > 0$, we understand that domain G is located to the right of the domain G_0. We denote hyper-plane – shared border of domains G_0 and G – as H:

$$H = \{(x, y) \mid x = 0, y \in D\} \equiv \left(\bar{G}_0 \cap \bar{G}\right) \setminus \partial D .$$

Right border of the domain G_0 is denoted as H_0:

$$H_0 = \{(x, y) \mid x = -\delta, y \in \bar{G}_0\} .$$

We will use notation $x = 0$ and $x = -\delta$ for hyper-planes H and H_0.

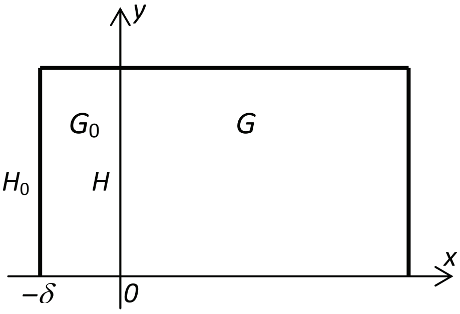

Fig. 1.4: General geometry of the domain

Let us call functions $U_0(x, y)$ and $U(x, y)$ as solution of original problem if they are continuous in corresponding domains $\bar{G}_0$, $\bar{G}$ and fulfil following equations:

a) differential equations:

$$\frac{\partial}{\partial x}\left(k_0 \frac{\partial U_0}{\partial x}\right) + \mathcal{L}_0\left(U_0\right) = -F_0(x, y) , \tag{21}$$

$$\frac{\partial}{\partial x}\left(k \frac{\partial U}{\partial x}\right) + \mathcal{L}\left(U\right) = -F(x, y) , \tag{22}$$

where $\mathcal{L}_0$ and $\mathcal{L}$ are differential operators;

b) conjugation conditions:

$$U_0\big|_{x=0} = U\big|_{x=0} , \tag{23}$$

$$k_0 \frac{\partial U_0}{\partial x}\bigg|_{x=-0} = k \frac{\partial U}{\partial x}\bigg|_{x=+0} ; \tag{24}$$

c) Neumann boundary condition on border H_0:

$$-k_0 \frac{\partial U_0}{\partial x}\bigg|_{x=-\delta} = \phi^0(y) ; \tag{25}$$

d) boundary conditions on the rest borders that are not necessary to concretize at this moment:

$$\tilde{\ell}\left(\tilde{U}\right) = \tilde{\Psi}(x, y) ,\ (x, y) \in \partial\tilde{D} = \partial D \setminus H_0 . \tag{26}$$

Here, $\tilde{\ell}$ is differential operator; function $\tilde{U}(x, y)$ is defined to be equal to function $U_0(x, y)$ in domain $\bar{G}_0$ and – to be equal to $U(x, y)$ in domain $\bar{G}$. It is continuous in $\bar{D}$ because of equation (23).

We require that all derivatives of equation (21) are continuous in domain G_0 and derivatives of equation (22) – in domain G. Derivative $\partial\tilde{U}/\partial x$ is continuous function in domain D except hyper-plane H where it has the first kind discontinuity and condition (24) is fulfilled. Note that value δ is comparatively small but still finite – averaging will not be made by tending it to the limit $\delta \to 0$.

We assume that coefficient k_0 and coefficients of the differential operator $\mathcal{L}_0$ are not dependent on argument x but could be dependent on argument y. Besides, operator $\mathcal{L}_0$ is linear and it do not contain derivatives regarding the argument x.

Let us see two examples of operators $\mathcal{L}_0$ and $\mathcal{L}$:

1) operators for 1D (in space) heat transfer problem:

$$\mathcal{L}_0\left(U_0\right) = -c_0\rho_0 \frac{\partial U_0}{\partial t}, \tag{27}$$

$$\mathcal{L}\left(U\right) = -c\rho \frac{\partial U}{\partial t}; \tag{28}$$

2) operators for steady-state 3D heat transfer:

$$\mathcal{L}_0\left(U_0\right) = \frac{\partial}{\partial y}\left(k_0 \frac{\partial U_0}{\partial y}\right) + \frac{\partial}{\partial z}\left(k_0 \frac{\partial U_0}{\partial z}\right), \tag{29}$$

$$\mathcal{L}\left(U\right) = \frac{\partial}{\partial y}\left(k_1 \frac{\partial U}{\partial y}\right) + \frac{\partial}{\partial z}\left(k_1 \frac{\partial U}{\partial z}\right). \tag{30}$$

Let us obtain estimate of derivative $\partial U_0 / \partial x$. We expand it to Taylor series near point $x = 0$ and take into account conjugation condition (24):

$$\frac{\partial U_0}{\partial x} = \frac{k}{k_0} \frac{\partial U}{\partial x}\bigg|_{x=+0} + x \frac{\partial^2 U_0}{\partial x^2}\bigg|_{x=-0} + O(x^2), \quad x \in [-\delta, 0].$$

From here, such estimate is valid [3]:

$$\max_{x\in[-\delta,0]} \left|\frac{\partial U_0}{\partial x}\right| \le \frac{k}{k_0} \left|\frac{\partial U}{\partial x}\right|_{x=+0} + \delta \max_{x\in[-\delta,0]} \left|\frac{\partial^2 U_0}{\partial x^2}\right| + O(\delta^2).$$

It shows that alteration of values of the solution U_0 is comparatively small in the direction of argument x if coefficient k_0 is significantly larger than k or if δ is small (or both conditions take place). That means that function $U_0(x,y)$ could be approximately substituted by constant regarding argument x with accuracy $O\left(\delta k/k_0 + \delta^2\right)$. Otherwise, substitution by constant in the x-direction could be inappropriate – polynomial or exponential approximation should be used.

1.2.2 Transformed Problem with Non-Classical Boundary Condition

We will convert differential equation (21) to non-classical boundary condition for the equation (22). It means that we will have other mathematical problem instead of the problem (21)-(26). To make difference between these two problems clearer, we denote the new solution of the equation (22) as $u(x, y)$ instead of the function $U(x, y)$.

We rewrite equation (22):

$$\frac{\partial}{\partial x}\left(k \frac{\partial u}{\partial x}\right) + \mathcal{L}\left(u\right) = -F(x, y), \ (x, y) \in G; \tag{31}$$

and introduce integral averaged value function:

$$u_0(y) = \frac{1}{\delta}\int_{-\delta}^{0} U_0(x, y)dx\,. \tag{32}$$

After integrating equation (21) over the segment $[-\delta, 0]$ and taking into account conjugation condition (24), we obtain:

$$k\frac{\partial u}{\partial x}\bigg|_{x=+0} - k_0\frac{\partial U_0}{\partial x}\bigg|_{x=-\delta} + \delta\mathcal{L}_0\left(u_0\right) = -\delta f_0\,, \tag{33}$$

where $f_0(y)$ is averaged value of the source function:

$$f_0(y) = \frac{1}{\delta}\int_{-\delta}^{0} F_0(x, y)dx\,. \tag{34}$$

Equation (33) is not a valid boundary condition yet because it has two unknown functions: $U_0(-\delta, y)$ and $u_0(y)$. We use boundary condition (25) to exclude function U_0 from the equation (33):

$$k\frac{\partial u}{\partial x}\bigg|_{x=+0} + \delta\mathcal{L}_0\left(u_0\right) = -\left(\phi^0 + \delta f_0\right). \tag{35}$$

1.2.2.1 Approximation by Constant

To move forward, we need to approximate function $U_0(x,y)$ in respect to argument x. Accuracy of this depends on particular task. We start with simplest one – approximation by constant. Taking into account expressions (23) and (32), we get:

$$U_0\left(x, y\right) = u_0(y) = u(0, y)\,. \tag{36}$$

New boundary condition is found if we put this equality into equation (15):

$$k\frac{\partial u}{\partial x}\bigg|_{x=+0} + \delta\mathcal{L}_0\left(u\big|_{x=0}\right) = -\left(\phi^0 + \delta f_0\right). \tag{37}$$

So, the transformed problem consists of differential equation (31), non-classical boundary condition (37) on the border H and original boundary conditions (26) on the other borders. New problem is defined in the sub-domain G of the initial domain D (Fig. 1.5).

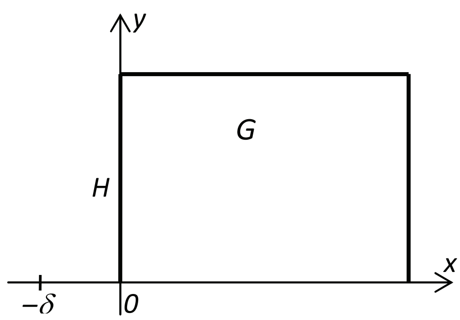

Fig. 1.5: Domain of the transformed problem

To be correct, we need also to add boundary condition on the borders of the hyper-plane H:

$$\boldsymbol{\ell}_0\left(u\right)=\psi_0(y)\,,\ y\in\partial H\,; \tag{38}$$

where operator $\boldsymbol{\ell}_0$ is defined in domain $\partial\tilde{D}\cap G_0$ and is equal to operator $\tilde{\boldsymbol{\ell}}$ here; ψ_0 is analogue of averaged value integral (32) for the function Ψ_0:

$$\psi_0(y):=\frac{1}{\delta}\int_{-\delta}^{0}\Psi_0(x,y)dx\,.$$

Ψ_0 in its turn is G_0 part of the function $\tilde{\Psi}$.

If function ϕ^0 is not identical to zero, boundary condition (25) and assumption of independency of x are true only for $k_0=\infty$. That means that approximation of argument x of function U_0 by constant is applicable if values of coefficient k_0 is relevantly large.

1.2.2.2 Linear Approximation

If we apply linear approximation to the function $U_0(x,y)$ in direction of x axis

$$U_0(x,y)=u_1(y)+xu_2(y) \tag{39}$$

and use conjugation condition (23) and boundary condition (25), we obtain

$$U_0(x,y)=u(0,y)+\frac{x}{k_0}\phi^0(y)\,. \tag{40}$$

Now we apply integral (32) to the expression (40) and put the result into equation (35) to get boundary condition on the border H:

$$k\left.\frac{\partial u}{\partial x}\right|_{x=+0}+\delta\boldsymbol{\mathcal{L}}_0\left(\left.u\right|_{x=0}\right)=-\phi_1\,; \tag{41}$$

where $\phi_1=\phi^0+\delta f_0+\tfrac{1}{2}\delta^2\boldsymbol{\mathcal{L}}_0\left(\phi^0/k_0\right)$. (42)

After finding solution $u(x,y)$, we can approximately restore function $U_0(x,y)$ by formula (40).

1.2.2.3 Approximation by Second-Degree Polynomial

We assume representation of the function U_0 as follows:

$$U_0(x,y)=u(0,y)+\frac{x}{\delta}u_1(y)+\left(\frac{x}{\delta}\right)^2u_2(y)\,. \tag{43}$$

Conjugation condition (24) gives:

$$k\left.\frac{\partial u}{\partial x}\right|_{x=+0}=\frac{k_0}{\delta}u_1(y)\,. \tag{44}$$

From the condition (25) and integral (32), we obtain:

$$\frac{k^0}{\delta}(2u_2-u_1)=\phi^0\,, \tag{45}$$

$$u_0=\left.u\right|_{x=0}-\tfrac{1}{2}u_1+\tfrac{1}{3}u_2\,. \tag{46}$$

After writing down u_1 and u_2 in terms of u_0, we can transform equation (44):

$$k\left.\frac{\partial u}{\partial x}\right|_{x=+0} = \frac{3k_0}{\delta}\left(u|_{x=0} - u_0\right) + \frac{\phi^0}{2}. \tag{47}$$

Now, we need only to express u_0 from this equation and put it into (35) to get boundary condition on the border H:

$$k\frac{\partial u}{\partial x} + \delta\mathcal{L}_0\left(u - \frac{\delta k}{3k_0}\frac{\partial u}{\partial x}\right) = -\phi_2 \tag{48}$$

where $\phi_2 = \phi^0 + \delta f_0 + \frac{1}{6}\delta^2\mathcal{L}_0(\phi^0/k_0)$. (49)

For calculating purposes, it could be useful to leave boundary condition in the form of the system. Then it would contain equations (35) and (47). If we put formula (47) into (35), we could use following form for the second equation of the system as well:

$$\delta\mathcal{L}_0(u_0) + \frac{3k_0}{\delta}\left(u|_{x=0} - u_0\right) = -\left(\tfrac{3}{2}\phi^0 + \delta f_0\right). \tag{50}$$

We can also use formulae (47) and (50) together as the system of equation on the boundary $x = 0$.

1.2.2.4 Exponential Approximation

Let us assume another representation for the function U_0:

$$U_0(x,y) = u(0,y) + \left(\mathrm{e}^{-qx/\delta} - 1\right)u_1(y) + \left(1 - \mathrm{e}^{qx/\delta}\right)u_2(y) \tag{51}$$

where parameter $q > 0$ is arbitrary (positive) constant. It could be freely chosen taking into account physical and geometrical properties of particular problem. Simplest way is to take $q = 1$.

We get boundary condition on the border H using similar mathematical modification as in previous case:

$$k\left.\frac{\partial u}{\partial x}\right|_{x=+0} + \delta\mathcal{L}_0\left(u|_{x=0} - C_1\frac{\delta k}{k_0}\left.\frac{\partial u}{\partial x}\right|_{x=+0}\right) = -\phi_3 \tag{52}$$

where $\phi_3 = \phi^0 + \delta f_0 + C_2\delta^2\mathcal{L}_0\left(\dfrac{\phi^0}{k_0}\right)$. (53)

Values of the parameters C_1, C_2 depend on choice of parameter q:

$$C_1(q) = \frac{\mathrm{e}^{2q}(q-1) + q + 1}{q^2\left(\mathrm{e}^{2q} - 1\right)}, \tag{54}$$

$$C_2(q) = \frac{\mathrm{e}^{2q} - 2q\,\mathrm{e}^{q} - 1}{q^2\left(\mathrm{e}^{2q} - 1\right)}. \tag{55}$$

Again, we can use system on the boundary $x = 0$. First equation of the system is (35) and the second is the following:

$$k\left.\frac{\partial u}{\partial x}\right|_{x=+0} = \frac{k_0}{C_1\delta}\left(u|_{x=0} - u_0\right) + \frac{C_2}{C_1}\phi^0 \tag{56}$$

or $$\delta \mathcal{L}_0(u_0)+\frac{k_0}{C_1\delta}\left(u\big|_{x=0}-u_0\right)=-\left(\left(1+\frac{C_2}{C_1}\right)\phi^0+\delta f_0\right). \qquad (57)$$

1.2.3 Error Estimates for Transformed Problem

Let us obtain an error estimate that occurs when initial problem is replaced with transformed problem. We decompose function $U_0(x,y)$ to Taylor series at the point $x=0$ under fixed argument y and take first three additives. Let us denote this by $\bar{U}_0$:

$$\bar{U}_0(x,y)=\left[U_0-x\frac{\partial U_0}{\partial x}+\frac{x^2}{2}\frac{\partial^2 U_0}{\partial x^2}\right]_{x=-0}. \qquad (58)$$

If we apply conjugation conditions (23), (24) to the first two additives of expression (58) and differential equation (21) to the third additive, we obtain:

$$\bar{U}_0(x,y)=u\big|_{x=0}-x\frac{k}{k_0}\frac{\partial u}{\partial x}\bigg|_{x=+0}-\frac{x^2}{2k_0}\left(\mathcal{L}_0(u)+F_0\right)\big|_{x=-0}. \qquad (59)$$

We define error in interval $x\in(-\delta,0)$:

$$\Delta U_0(x,y)=\left|\bar{U}_0(x,y)-\bar{\bar{U}}_0(x,y)\right| \qquad (60)$$

where $\bar{\bar{U}}_0$ is approximate solution of U_0 what we obtain after solving transformed problem. If we use constant approximation in conservative averaging method, function $\bar{\bar{U}}_0$ is expressed by equality (36). In case of linear approximation, formula (40) is used. If we continue, expression for the second-degree polynomial approximation is

$$\bar{\bar{U}}_0(x,y)=u\big|_{x=0}+x\frac{k}{k_0}\left(1+\frac{x}{2\delta}\right)\frac{\partial u}{\partial x}\bigg|_{x=+0}+x^2\frac{\phi^0}{2\delta k_0} \qquad (61)$$

and – for exponential approximation (when $q=1$):

$$\bar{\bar{U}}_0=u\big|_{x=0}+\frac{\delta}{(\mathrm{e}^2-1)k_0}\left(\mathrm{e}^2(1-\mathrm{e}^{\frac{x}{\delta}})-\mathrm{e}^{-\frac{x}{\delta}}+1\right)\left(-k\frac{\partial u}{\partial x}\bigg|_{x=+0}+\frac{\mathrm{e}^2-2\mathrm{e}-1}{2}\phi^0\right). \qquad (62)$$

Let us estimate an error at the point $x=-\delta$ if approximation with constant is used:

$$\Delta U_0\le\frac{\delta}{k_0}\left[k\left|\frac{\partial u}{\partial x}\right|+\frac{\delta}{2}\left|\mathcal{L}_0(u)+F_0\right|\right]_{x=0}. \qquad (63)$$

Similarly, we can obtain estimates for other kinds of approximation, for example, second-degree polynomial:

$$\Delta U_0\le\frac{\delta}{2k_0}\left[3k\left|\frac{\partial u}{\partial x}\right|+\delta\left|L^0(u)+F_0\right|+\left|\phi^0\right|\right]_{x=0}; \qquad (64)$$

or exponential approximation:

$$\Delta U_0\le\frac{\delta}{k_0}\left[\frac{2k}{\mathrm{e}+1}\left|\frac{\partial u}{\partial x}\right|+\frac{\delta}{2}\left|L^0(u)+F_0\right|+\frac{(\mathrm{e}-1)^3}{\mathrm{e}+1}\left|\phi^0\right|\right]_{x=0}. \qquad (65)$$

We can see from estimates that error of averaging reduces if increases discontinuity of coefficients k and k_0. Error decreases also if thickness of the layer δ is decreased.

This is unlike other – classical methods where increasing of discontinuity of coefficients leads to additional difficulties and greater error.

1.2.4 Usage of the Method in the Case of the Dirichlet Boundary Condition

Consider Dirichlet condition instead of (25) on the boundary H_0:

$$U_0\big|_{x=-\delta} = \varphi^0(y)\,. \tag{66}$$

1.2.4.1 Approximation by Constant

If we directly transfer boundary condition from boundary H_0 to H: $u(0,y)=\varphi^0(y)$, we lose solution dependence on parameters k_0, F_0 and δ. Therefore, we use equation (33) to obtain boundary condition on H. The second additive of the equation is zero because U_0 is not dependent on argument x, but, in the third additive, we replace u_0 by φ^0. We get:

$$k\frac{\partial u}{\partial x} = -\delta\left(f_0 + \mathcal{L}_0(\varphi^0)\right). \tag{67}$$

Evidently, Dirichlet boundary condition on the boundary H_0 changed to Neumann condition on the boundary H. Condition (67) changes to non-classical form if we, instead of $u_0 = \varphi^0$, use averaged value $u_0 = \frac{1}{2}\left(u+\varphi^0\right)$ in operator $\mathcal{L}_0$ of equation (33):

$$k\frac{\partial u}{\partial x} + \frac{\delta}{2}\mathcal{L}_0(u) = -\delta\left(f_0 + \frac{1}{2}\mathcal{L}_0(\varphi^0)\right). \tag{68}$$

1.2.4.2 Linear Approximation

Approximation of U_0 by linear function over argument x gives such obvious expressions:

$$u_0 = \tfrac{1}{2}\left(u(0,y) - \varphi^0\right), \tag{69}$$

$$k_0\frac{\partial U_0}{\partial x}\bigg|_{x=-\delta} = \frac{k_0}{\delta}\left(u(0,y) - \varphi^0(y)\right). \tag{70}$$

If we use them in equation (33), we get following boundary condition on H:

$$u - \delta\frac{k}{k_0}\frac{\partial u}{\partial x} + \frac{\delta^2}{2k_0}\mathcal{L}_0(u) = \varphi^0 + \frac{\delta^2}{k_0}\left(f_0 + \frac{1}{2}\mathcal{L}_0(\varphi^0)\right). \tag{71}$$

It is visible that this condition is close to Dirichlet condition if δ is small and k_0 is relatively large in comparison with k.

1.2.4.3 Approximation by Polynomial

If we approximate U_0 by polynomial expression (43), we can obtain unknown coefficients u_1(y), u_2(y) using conjugation condition (23), boundary condition (66) and integral (32):

$$u_1 = 4u\big|_{x=0} + 2\varphi^0 - 6u_0\,,\; u_2 = 3u\big|_{x=0} + 3\varphi^0 - 6u_0\,. \tag{72}$$

It is possible to express u_0 using $\partial u/\partial x$:

$$u_0 = \frac{1}{3}\left[2u + \varphi^0 - \frac{\delta k}{2k_0}\frac{\partial u}{\partial x}\right]_{x=0}. \tag{73}$$

From here, we get required boundary condition on the boundary H of the transformed problem:

$$u - \delta\frac{k}{k_0}\frac{\partial u}{\partial x} - \frac{\delta^2}{3k_0}\mathcal{L}_0\left(u - \frac{\delta k}{4k_0}\frac{\partial u}{\partial x}\right) = \varphi^0 + \frac{\delta^2}{2k_0}\left(f_0 + \frac{1}{3}\mathcal{L}_0(\varphi^0)\right). \tag{74}$$

Similarly as in section 1.2.2.3, condition on the boundary H could be left in the form of system:

$$\frac{\delta k}{2k_0}\frac{\partial u}{\partial x} = 2u - 3u_0 + \varphi^0, \tag{75}$$

$$u - 2\left(u_0 - \varphi^0\right) + \frac{\delta^2}{6k^0}\mathcal{L}_0(u_0) = \varphi^0 - \frac{\delta^2}{2k_0}f_0. \tag{76}$$

1.2.4.4 Exponential Approximation

We assume that function U_0 is in form (51). We can obtain unknown functions u_1 and u_2 if we use expressions (24), (32), (66). After that, equation (33) can be transformed to the boundary condition on the border H. If parameter q = 1, condition is:

$$u - \frac{2\delta k C_3}{k_0}\frac{\partial u}{\partial x} - \frac{2\delta^2}{k_0 C_3}\mathcal{L}_0(u) - \frac{\delta^3 k C_4}{k_0^2}\mathcal{L}_0\left(\frac{\partial u}{\partial x}\right) = \varphi^0 + \frac{\delta^2}{k_0}\left(C_3 f_0 + C_5\mathcal{L}_0\left(\varphi^0\right)\right) \tag{77}$$

where constants are as follows:

$$C_3 = (\mathrm{e}-1)/(\mathrm{e}+1),\ C_4 = (\mathrm{e}^2-4\mathrm{e}+3)/(\mathrm{e}^2-1),\ C_5 = (\mathrm{e}^2-2\mathrm{e}-1)/(\mathrm{e}^2+1).$$

Error estimates could be obtained similarly as above – using Taylor series. The exception is the case of constant approximation:

$$\Delta\bar{\bar{U}}_0 \le \left|u(0,y) - \varphi^0(y)\right|. \tag{78}$$

1.2.5 Usage of the Method in the Case of the Robin Boundary Condition

Consider such condition on boundary H_0:

$$\left.\left(-k_0\frac{\partial U_0}{\partial x} + h_0 U_0\right)\right|_{x=-\delta} = \varphi^0(y). \tag{79}$$

Approximation of function U_0 by constant, expression (33) and fact that $u_0(y) = U_0(x,y) = u(0,y)$, gives:

$$-k\frac{\partial u}{\partial x} + h_0 u - \delta\mathcal{L}_0(u) = \varphi^0 + \delta f. \tag{80}$$

If we assume linear dependence of function U_0 on argument x:

$$U_0(x,y) = u(0,y) + xu_1(y); \tag{81}$$

and take into account formulae (32), (33) and (79), new boundary condition is:

$$-k\frac{\partial u}{\partial x}+\frac{k_0 h_0}{\tilde{k}}u-\delta\mathcal{L}_0\left(\left(1-\frac{\delta h_0}{2\tilde{k}}\right)u\right)=\varphi_1; \tag{82}$$

where $\tilde{k}=k_0+\delta h_0$ and

$$\varphi_1=\frac{k_0}{\tilde{k}}\varphi^0+\delta f_0+\mathcal{L}_0\left(\frac{\delta^2}{2\tilde{k}}\varphi^0\right). \tag{83}$$

Approximation of function U_0 by polynomial of the second order leads to the following equation:

$$-\frac{k\tilde{k}}{k_0}\frac{\partial u}{\partial x}+h_0 u-\frac{\delta}{3k_0}\mathcal{L}_0\left[\left(3k_0+\delta h_0\right)u-\delta k\left(1+\frac{\delta h_0}{4k_0}\right)\frac{\partial u}{\partial x}\right]=\varphi_2; \tag{84}$$

where $\varphi_2=\varphi^0+\delta\left(1+\frac{\delta h_0}{2k_0}\right)f_0+\frac{\delta^2}{6k_0}\mathcal{L}_0(\varphi^0)$. (85)

As before, boundary condition in case of polynomial approximation can be written as system of two equations that contain averaged value function u_0.

If exponential approximation (51) is used, equation (33) gives condition on $x=0$:

$$k\frac{\partial u}{\partial x}-k_0\left(\mathrm{e}^q u_1+\mathrm{e}^{-q}u_2\right)+\delta\mathcal{L}_0\left(u_0\right)=-\delta f_0. \tag{86}$$

We find unknown functions $u_1(y)$ and $u_2(y)$ from boundary condition (79) and conjugation condition (24):

$$u_1(y)=\frac{1}{\gamma}\left(-\delta h_0 u+\left(qk_0\,\mathrm{e}^{-q}+h_0\left(1-\mathrm{e}^{-q}\right)\right)\frac{\delta k}{qk_0}\frac{\partial u}{\partial x}+\delta\varphi^0\right), \tag{87}$$

$$u_2(y)=-\left(u_1(y)+\frac{\delta k}{qk_0}\frac{\partial u}{\partial x}\right), \tag{88}$$

$$\gamma=2\left(qk_0\sinh(q)+\delta h_0\left(\cosh(q)-1\right)\right).$$

Average value function $u_0(y)$ is obtained by integral (32):

$$u_0=u\big|_{x=0}-u_1\left(1+\frac{1-\mathrm{e}^q}{q}\right)+u_2\left(1-\frac{1-\mathrm{e}^{-q}}{q}\right). \tag{89}$$

1.3 Polar and Cylindrical Coordinate System

1.3.1 Original Problem

Let us take cylindrical domain $D=G_0\cup G\cup H$, $G_0\cap G\cap H=\varnothing$ (Fig. 1.6):

$$(r,y)\in\bar{D}\subset R^4,\ r\in R,\ y=(\phi,z,t)\in R^3,$$

$$G_0=\{(r,y)\,|\,r\in(\tilde{r}_0,r_0),y\in D\},\quad G=\{(r,y)\,|\,r\in(r_0,r_1),y\in D\},$$

$$H_0=\{(r,y)\,|\,r=\tilde{r}_0,y\in\bar{G}_0\},\quad H=\{(r,y)\,|\,r=r_0,y\in D\}\equiv\left(\bar{G}_0\cap\bar{G}\right)\setminus\partial D.$$

Argument r represents radius, but y could be also with less dimensions, depending on particular mathematical model, e.g., $y=(z,t)$, $y=(\phi,z)$ or $y=(z)$. Similarly as in previous section, we denote domain (surface) H_0 as $r=\tilde{r}_0$ and domain H – as $r=r_0$.

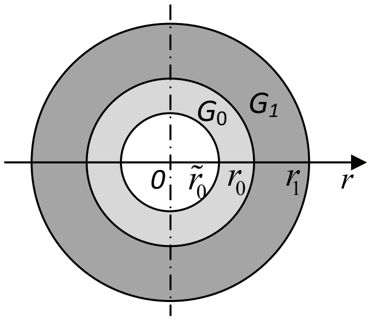

Fig. 1.6: Circular domain of the original problem

We have:

a) differential equations for domains G_0 and G:

$$\frac{1}{r}\frac{\partial}{\partial r}\left(rk_0\frac{\partial U_0}{\partial r}\right)+\mathcal{L}_0\left(U_0\right)=-F_0(r,y)\,, \tag{90}$$

$$\frac{1}{r}\frac{\partial}{\partial r}\left(rk\frac{\partial U}{\partial r}\right)+\mathcal{L}\left(U\right)=-F(r,y)\,; \tag{91}$$

where $\mathcal{L}_0$ is linear differential operator that is not dependent on argument r;

b) conjugation conditions:

$$U_0\Big|_{r=r_0}=U\Big|_{r=r_0}\,, \tag{92}$$

$$k_0\frac{\partial U_0}{\partial r}\bigg|_{r=r_0-0}=k\frac{\partial U}{\partial r}\bigg|_{r=r_0+0}\,; \tag{93}$$

c) boundary condition at $r=\tilde{r}_0$:

$$r\frac{\partial U_0}{\partial r}\bigg|_{r=\tilde{r}_0}=\varphi_0(y)\,. \tag{94}$$

This condition is used in such form if domain is a ring or cored cylinder.

Boundary condition is homogeneous if $\tilde{r}_0=0$ (Fig. 1.7):

$$r\frac{\partial U_0}{\partial r}\bigg|_{r=0}=0\,; \tag{95}$$

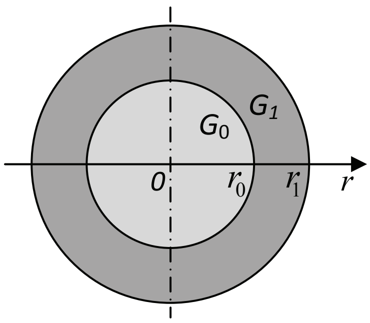

Fig. 1.7: Domain with a full core

d) boundary conditions on other borders:

$$\tilde{\boldsymbol{\ell}}(\tilde{U}) = \tilde{\Psi}(r, y),\ (r, y) \in \partial\tilde{D} = \partial D \setminus H_0\,; \tag{96}$$

where function $\tilde{U}(r, y)$ is defined similarly as in previous section, i.e., it is equal to $U_0(r, y)$ or $U(r, y)$ in corresponding sub-domains.

1.3.2 Transformed Problem

Let us apply conservative averaging method to the sub-domain G_0 that is located closer to the center of the domain D. Solution of transformed problem we denote as $u(r, y)$ that is defined in domain G. We rewrite equation (92) with new notation:

$$\frac{1}{r}\frac{\partial}{\partial r}\left(rk\frac{\partial u}{\partial r}\right) + \boldsymbol{\mathcal{L}}(u) = -F(r, y)\,. \tag{97}$$

Again, we introduce integral averaged value function that is different from equation (12) because of cylindrical coordinates:

$$u_0(y) = \frac{2}{r_0^2 - \tilde{r}_0^2}\int_{\tilde{r}_0}^{r_0} rU_0(r, y)dr\,. \tag{98}$$

For simplicity, we will consider only the case $\tilde{r}_0 = 0$ in further transformations.

We integrate equation (90) over the segment $[0, r_0]$ and take into account conjugation condition (93):

$$\left.\frac{2k}{r_0}\frac{\partial u}{\partial r}\right|_{r=r_0+0} + \boldsymbol{\mathcal{L}}_0(u_0) = -f_0(y)\,; \tag{99}$$

where f_0 is averaged value function of source function F_0:

$$f_0(y) = \frac{2}{r_0^2}\int_0^{r_0} rF_0(r, y)dr\,. \tag{100}$$

We will use equality (99) to obtain non-classical boundary condition for the equation (97) on the border $r = r_0$. (Fig. 1.8)

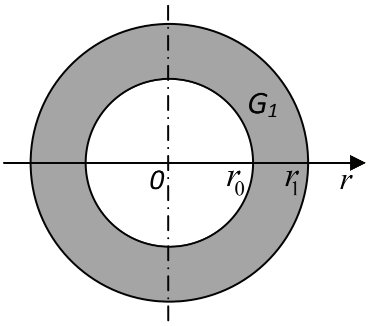

Fig. 1.8: Ring-shaped domain of the transformed problem

1.3.2.1 Approximation by Constant

Let us assume that function U_0 is constant over argument r. Taking into account conjugation condition (92), we find boundary condition on the border $r = r_0$:

$$\frac{2k}{r_0}\frac{\partial u}{\partial r}\bigg|_{r=r_0+0} + \mathcal{L}_0(u|_{r=r_0}) = -f_0(y)\,. \tag{101}$$

Approximation with linear function leads to the same equation because of boundary condition (95) at the point $r = 0$.

1.3.2.2 Approximation by Second-Degree Polynomial

We assume such representation for the function U_0:

$$U_0(r,y) = u_1(y) + ru_2(y) + r^2u_3(y)\,. \tag{102}$$

Conjugation conditions (92), (93) and boundary condition (95) allow us to find unknown functions u_1, u_2, u_3. This allows rewriting the expression for the temperature U_0 as follows:

$$U_0(r,y) = u_0 + \left(\frac{2r^2}{r_0^2} - 1\right)\left(u|_{r=r_0} - u_0\right). \tag{103}$$

Here $u_0(y) = u|_{r=r_0} - \dfrac{r_0 k}{4k_0}\dfrac{\partial u}{\partial r}\bigg|_{r=r_0+0}$. (104)

The equality (99) gives the first boundary equation:

$$\frac{8k_0}{r_0^2}\left(u|_{r=r_0} - u_0\right) + \mathcal{L}_0(u_0) = -f_0\,. \tag{105}$$

Derivation of function (103) by argument r and putting the result into conjugation condition (93) gives the second equation on the boundary $r = r_0$:

$$k\frac{\partial u}{\partial r}\bigg|_{r=r_0+0} = \frac{4k_0}{r_0}\left(u|_{r=r_0} - u_0\right). \tag{106}$$

New formulation of the problem consists of differential equation (97), boundary conditions (105), (106) on the border $r = r_0$ and original boundary conditions on the other borders of the domain G. After solving this problem, we can find approximation for the function $U_0(r, t)$ from (103).

1.3.2.3 Exponential Approximation

We assume following representation for function U_0:

$$U_0(r,y) = u_1(y) + (\mathrm{e}^{-r/r_0} - 1)u_2(y) + (1 - \mathrm{e}^{r/r_0})u_3(y)\,. \tag{107}$$

We can obtain unknown functions u_1, u_2, u_3 and write down function U_0 after using boundary condition (70) and both conjugation conditions:

$$U_0(r,y) = u|_{r=r_0} + \frac{r_0 k}{\sinh(1)k_0}\frac{\partial u}{\partial r}\bigg|_{r=r_0+0}\left(\cosh(r/r_0) - \cosh(1)\right). \tag{108}$$

In this case, integral averaged value function is given by expression

$$u_0(y) = u|_{r=r_0} - \frac{r_0 k}{C_0 k_0}\frac{\partial u}{\partial r}\bigg|_{r=r_0+0}, \tag{109}$$

where constant $C_0 = (\mathrm{e}^2 - 1)/(\mathrm{e}^2 - 4\mathrm{e} + 5)\,.$ (110)

This is the first equation on the border $r = r_0$. We find the second one by using equality (99):

$$\frac{2C_0k_0}{r_0^2}\left(u\big|_{r=r_0} - u_0\right) + \mathcal{L}_0(u_0) = -f_0\,. \tag{111}$$

After finding solution, we can approximately reconstruct values in the domain G_0 by formula (108). Function U_0 could be expressed also in terms of u_0 that is more convenient for calculation purposes:

$$U_0(r,y) = u\big|_{r=r_0} + \beta_0(r)\left(u\big|_{r=r_0} - u_0\right) \tag{112}$$

where $\beta_0(r) = \dfrac{2\,\mathrm{e}}{\mathrm{e}^2 - 4\,\mathrm{e} + 5}\left(\cosh\dfrac{r}{r_0} - \cosh(1)\right)$. (113)

1.4 Conclusions

The theoretical basis of the conservative averaging method was considered in this chapter. At the beginning, the main concept with an example was given. It was written as a simple introduction of the method for interested persons, and could also be used as teaching aid for students. Next, a general description of conservative averaging in Cartesian and polar coordinates using polynomial, exponential and constant approximation was presented. Although the conservative averaging method has been used for several decades, there are still many theoretical aspects that wait to be researched.

2 Heat Transfer in Cylindrical Wire with Insulation

Calculation of heat transfer and heat emission in electrical wires is a vital issue in many industries. Electric circuitry is used in cars, houses, consumer electronics, etc. Damage and accidents are possible if insulation melts because of heightened temperature in the wires. The thermal properties of conductor and insulation significantly differ, which makes calculation of critical temperatures more difficult.

In this chapter, a single round wire is considered. Since the length of the wire is much larger than diameter, 1D model is used as in [17]. The heat conductivity coefficient of the conductor is substantially greater in comparison with the coefficient of the insulation of the wire. In this situation, it is possible to use conservative averaging as a mesh reduction method which diminishes the domain of numerical calculation. In other words, it is sufficient to make calculations on the insulation of the wire, but the temperature distribution for the wire itself is estimated in an analytical way. If we compare with the mentioned paper [17], the finite volume method was used there to calculate the temperature in both regions – conductor and insulation.

2.1 Statement of the Problem

We have two-layer domain (Fig. 2.1) that consists of electrical conductor and insulation. We denote radius of metallic wire by r_0 and – outer radius of insulation by r_1. We have:

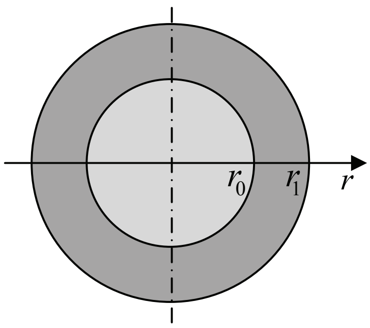

Fig. 2.1: Geometry of an insulated wire

a) heat transfer equation for conductor:

$$c_0 \frac{\partial U_0}{\partial t} = \frac{1}{r} \frac{\partial}{\partial r}\left(r k_0 \frac{\partial U_0}{\partial r} \right) + F_0(r,t), \quad r \in (0, r_0); \tag{1}$$

and homogeneous non-linear heat conduction equation for the insulation:

$$c \frac{\partial U}{\partial t} = \frac{1}{r} \frac{\partial}{\partial r}\left(r k \frac{\partial U}{\partial r} \right), \quad r \in (r_0, r_1); \tag{2}$$

b) conjugation conditions at $r = r_0$:

$$U_0\big|_{r=r_0} = U\big|_{r=r_0}, \tag{3}$$

$$k_0 \frac{\partial U_0}{\partial r}\bigg|_{r=r_0-0} = k\frac{\partial U}{\partial r}\bigg|_{r=r_0+0}; \tag{4}$$

c) boundary conditions:

$$r=0: \ \frac{\partial U_0}{\partial r}\bigg|_{r=0} = 0; \tag{5}$$

$$r=r_1: \ k\frac{\partial U}{\partial r}\bigg|_{r=r_1} + h(U|_{r=r_1} - \theta) = 0 \tag{6}$$

d) initial conditions:

$$t=0: \ U_0 = \theta, \ U = \theta. \tag{7}$$

Here c_0, c, k_0, k, h – temperature dependant coefficients which correspond to volumetric heat capacity, heat conductivity and heat exchange on the surface; θ – temperature of environment.

2.2 Transformed problem

We use conservative averaging method to exclude wire from definition domain – we will inspect heat transfer in the insulation only. We denote solution of the problem, which is transformed by conservative averaging method, as $u(r, t)$. New statement of the problem consists of differential equation (2) (replacing U by u), boundary condition (6), initial condition (7) and condition on the boundary $r = r_0$ that we will obtain from previous chapter. Differential operator $\mathcal{L}_0$ in our case is

$$\mathcal{L}_0(u) = -c_0 \frac{\partial}{\partial t}(u).$$

Boundary condition comes from formula (101) of the Chapter 1.3.2 if we use approximation by constant:

$$\frac{2k}{r_0}\frac{\partial u}{\partial r}\bigg|_{r=r_0+0} - c_0\frac{\partial}{\partial t}\left(u|_{r=r_0}\right) = -f_0(y); \tag{8}$$

formulae (105) and (106) are used for polynomial approximation:

$$\frac{8k_0}{r_0^2}\left(u|_{r=r_0} - u_0\right) - c_0\frac{\partial u_0}{\partial t} = -f_0, \tag{9}$$

$$k\frac{\partial u}{\partial r}\bigg|_{r=r_0+0} = \frac{4k_0}{r_0}\left(u|_{r=r_0} - u_0\right); \tag{10}$$

and formulae (109)-(111) – for exponential approximation:

$$u_0(y) = u|_{r=r_0} - \frac{r_0 k}{C_0 k_0}\frac{\partial u}{\partial r}\bigg|_{r=r_0+0}, \tag{11}$$

$$\frac{2C_0 k_0}{r_0^2}\left(u|_{r=r_0} - u_0\right) - c_0\frac{\partial u_0}{\partial t} = -f_0, \tag{12}$$

$$C_0 = \frac{\mathrm{e}^2 - 1}{\mathrm{e}^2 - 4\mathrm{e} + 5}. \tag{13}$$

2.3 Numerical Solution

Since it is not possible to obtain analytical solution for the stated problem because of non-linearity, we solve it in numerical way. We construct standard difference scheme with second order approximation regarding to r and first order approximation regarding to t.

As an example, we take wire of copper with polyvinylchloride (PVC) insulation. Coefficients in this case are as follows:

a) heat conductivity coefficient k_0 and k (W/m K)

$$k_0 = 401, \quad k = 0.2;$$

b) specific heat capacity coefficient c_0, c (W/m^3 K) as suggested in [16]

$$c_0(T) = 8960(381 + 0.17T),$$

$$c(T) = 1350(920 - 1.3T + 0.074T^2);$$

c) heat generation is achieved by electric current; direct current and ohm resistance is considered:

$$f_0(T) = \frac{I^2 \rho_{20}}{A^2}\left(1 + \alpha_{20}(T - 20)\right) \tag{14}$$

where I – electric current, A – cross sectional area of the metallic conductor, ρ_{20} – specific resistance of copper at reference temperature 20°C $\rho_{20} = 1.75 \cdot 10^{-8}\,\Omega$, α_{20} – temperature coefficient of copper resistance $\alpha_{20} = 3.9 \cdot 10^{-3} \cdot 1/\mathrm{K}$;

d) $h(T)$ – coefficient of the laminar unforced convection to air of the horizontal cylindrical surface is obtained from [26]. Computer subroutine from [16] was used for calculations. Range of coefficient's values is 3–20 if temperature range is 0–100°C and temperature of environment $\theta = 0$°C. All mentioned coefficients are valid in the temperature range of our interest. Temperature is given in centigrade degrees.

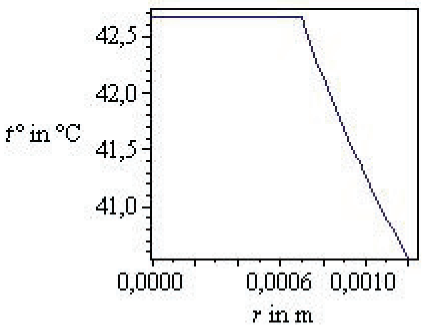

Fig. 2.2: Final temperature of Example 1

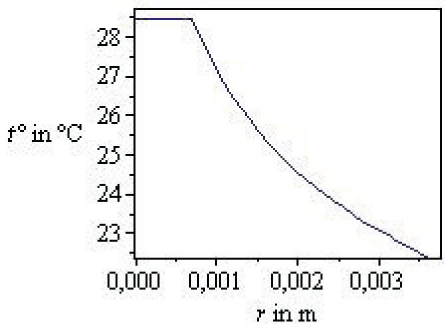

Fig. 2.3: Final temperature of Example 2

Fig. 2.2 shows temperature distribution after it becomes stable. Values of the parameters were used as follows: $r_0 = 0.7 \cdot 10^{-3}$ m, $r_1 = 1.2 \cdot 10^{-3}$ m, $\theta = 0$ °C, $I = 20$ A.

Graphics of solutions matches even if we use different approximations for function U_0. Largest difference is in the center of the wire, but only starting with fifth significant digit (see Table 2.1).

Approximation	Temperature
Constant approx.	42.66<u>46</u>°C
Polynomial approx.	42.66<u>57</u>°C
Exponential approx.	42.66<u>56</u>°C

Table 2.1: Temperature in the centre of a wire

Note that conservative averaging method does not make solution U linear as it is visually observed in Fig. 2.2. As an example, we can take outer radius 3 times larger: $r_1 = 3.6 \cdot 10^{-3}$ (Fig. 2.3). It is also numerically verified that we could choose such coefficients for stated problem that choice of approximation of U_0 by polynomial or exponential instead of constant is significant, but such parameters are useless from practical point of view.

2.4 Steady-State Analytical Solution

If the heat-up time of the wire is not important, a steady-state mathematical problem can be considered. Taking into account the results of the previous section, let us assume that the temperature in the wire is constant. It is equal to the temperature of the inner boundary of insulation if we assume continuity of temperature on that boundary. The domain of the problem corresponds to the insulation (Fig. 2.1).

Let us write down statement of the problem:

a) heat transfer equation in the insulation of the wire:

$$\frac{1}{r}\frac{d}{dr}\left(rk\frac{dU}{dr}\right)=0\,,\ U=U(r)\,,\ r\in(r_0,r_1)\,; \tag{15}$$

b) inner boundary receives heat that is generated by electric current in the conductor (f_0 as in formula (14) of the previous section):

$$r=r_0:\ \ k\frac{dU}{dr}+\frac{r_0}{2}f_0=0\,; \tag{16}$$

c) the same heat goes out from the outer surface of insulation:

$$r=r_1:\ \ k\frac{dU}{dr}+h(U-\theta)=0 \tag{17}$$

We can find analytical solution of the problem if coefficients k and h are constants. General solution of the ordinary differential equation is

$$U(r)=C_1+C_2\ln(r) \tag{18}$$

We can find unknown constants C_1 and C_2 by boundary conditions (16) and (17):

$$C_1=-C_2\left(\ln(r_1)+\frac{k}{r_1 h}\right)+\theta\,, \tag{19}$$

$$C_2=\frac{C_3\left(1+\alpha_{20}\left(\theta-20\right)\right)}{C_3\alpha_{20}\left(\ln\left(\frac{r_1}{r_0}\right)+\frac{k}{r_1\alpha}\right)-k}\ ,\quad C_3=\frac{I^2\rho_{20}}{2\pi^2 r_0^2} \tag{20}$$

In reality, heat convection coefficient h has non-linear dependence on the temperature of the surface, although it is possible to calculate temperature numerically by iterations. At first, coefficient h is calculated at an approximate temperature. The solution (18) gives a new value of the surface temperature which is used to calculate coefficient h again. The iterations are repeated while the result changes. The sufficient conditions to apply this procedure are stated in [27].

If we compare the steady-state solution with the example of the previous section, the results match (Fig. 2.2). A difference appears only with the 5th significant digit, which is negligible. For example, the temperature in the wire and on the inner surface of the insulation is 42.6648 °C that can be compared with results of the Table 2.1.

A steady-state solution does not exist if the generated heat is more than that given away by convection on the surface.

2.5 Conclusions

The conservative averaging method can be applied to stationary and non-stationary mathematical problems with transient coefficients. It enables the exclusion of a part of the original domain to reduce calculations. This model easily allows adding surface radiation by incorporating it in coefficient $h(T)$.

Experience shows that approximation by constant is sufficient in many practical heat transfer problems if one material has relatively large heat conductivity in comparison with the other one as was observed in the example of insulated wire. The numerical solution in the described model shows good conformity with recent results at Munich Bundeswehr University obtained by commercial software COMSOL that uses a 2D finite element method. Calculation of the mathematical model of conservative averaging is fast, and it allows the finding of solutions for different dimensions and materials quickly.

More complex electrical systems like wires combined in bundles are used in industrial applications often, and their mathematical models could be developed applying the conservative averaging in the future. Such and similar composed domains are examined using other mathematical methods, e.g., in the following recent papers: [28]-[31].

3 Cartesian Model of Automotive Fuse

Safety fuses are crucial elements of modern vehicles which preserve the safety of electrical equipment and car as a whole. Industrial companies have initiated research on this matter to meet tomorrow's demands of the precision of electric systems. Mathematical models are made to understand the existing behaviour of the fuses and to improve their design in the future.

Usually, mathematical modelling of fuses and similar objects is implemented by making one dimensional assumptions: [18], [32]-[34]. Here, the conservative averaging method is used to transform a 3D statement of the problem into a new type of statement that consists of three ordinary differential equations. An approximate analytical 3D solution is obtainable from the solution of the transformed problem afterwards. The number of dimensions corresponds to the count of space dimensions here. The additional time dimension is always present. The conservative averaging method is theoretically well founded for linear partial differential equations. As with [23] and the previous chapter, a quasi-linear mathematical problem is considered here.

3.1 Geometry of the Model

We start with geometric assumptions of typical car fuse (Fig. 3.1 and Fig. 3.2). We seemingly straighten out the fuse and use the geometry of the model as shown in Fig. 3.3. Because of the symmetry, it is enough to use only the shaded part of the model (Fig. 3.4 and Fig. 3.5).

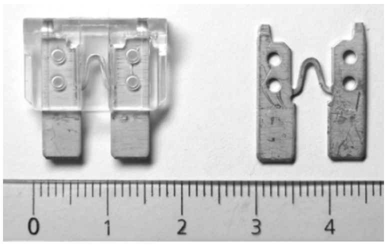

Fig. 3.1: Example of an automotive fuse with and without a plastic shell

Fig. 3.2: Examples of different automotive fuses

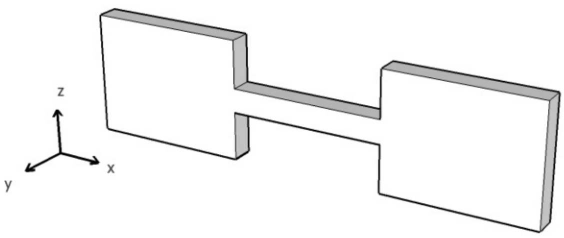

Fig. 3.3: Full geometry of the model

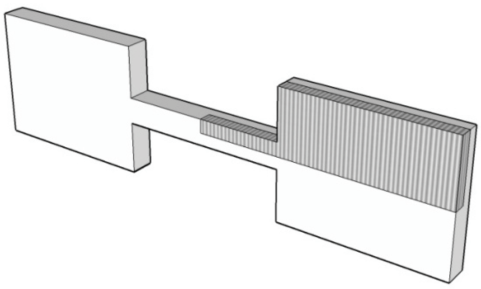

Fig. 3.4: Symmetry of the model

3.2 Mathematical Statement of the Original Problem

We continue with an accurate formulation of the three-dimensional mathematical model of the transient heat conduction problem for a fuse.

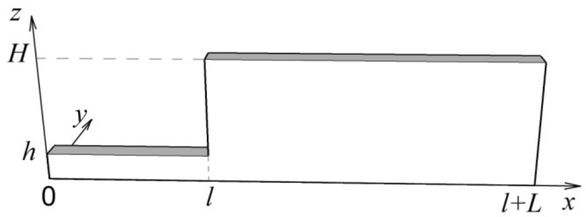

Fig. 3.5: Geometry of the domain

Let us treat main domain (Fig. 3.5) as two connected sub-domains G_0 and G_1:

$$G_0 = \{(x, y, z) \mid x \in [0, l], y \in [0, b], z \in [0, h]\},$$

$$G_1 = \{(x, y, z) \mid x \in [l, l+L], y \in [0, b], z \in [0, H]\}.$$

If temperature in the domain G_i is denoted as function $U_i\,(x, y, z, t)$, differential equation for the heat transfer is

$$\frac{\partial}{\partial t}(\gamma U_i) = \frac{\partial}{\partial x}\left(k\frac{\partial U_i}{\partial x}\right) + \frac{\partial}{\partial y}\left(k\frac{\partial U_i}{\partial y}\right) + \frac{\partial}{\partial z}\left(k\frac{\partial U_i}{\partial z}\right) + F_i(U_i), \tag{1}$$

$$U_i = U_i(x, y, z, t), \quad (x, y, z) \in G_i, \quad t > 0, \quad i = \overline{0,1}.$$

Source term F_i (heat produced by electric current) is approximated by linear function:

$$F_i(U_i) = B_i\left(1 + \alpha_r\left(U_i - U_r\right)\right); \tag{2}$$

where $B_0 = \dfrac{\rho_{ref} I^2}{h^2 b^2}$, $B_1 = \dfrac{\rho_{ref} I^2}{H^2 b^2}$.

Parameter ρ_{ref} is resistivity of the material at the reference temperature U_r, α_r is temperature coefficient of electric resistivity; I – electric current. Heat conductivity k and volumetric heat capacity γ depend on temperature.

Besides main equations (1), we add symmetry conditions:

$$\left.\frac{\partial U_0}{\partial x}\right|_{x=0} = 0, \quad \left.\frac{\partial U_0}{\partial y}\right|_{y=0} = 0, \quad \left.\frac{\partial U_0}{\partial z}\right|_{z=0} = 0, \tag{3}$$

$$\left.\frac{\partial U_1}{\partial x}\right|_{x=l+L} = 0, \quad \left.\frac{\partial U_1}{\partial y}\right|_{y=0} = 0, \quad \left.\frac{\partial U_1}{\partial z}\right|_{z=0} = 0; \tag{4}$$

and heat exchange conditions on outer surfaces:

$$\left.\left(k\frac{\partial U_0}{\partial y} + h_0\left(U_0 - \Theta\right)\right)\right|_{y=b} = 0, \qquad \left.\left(k\frac{\partial U_1}{\partial y} + h_1\left(U_1 - \Theta\right)\right)\right|_{y=b} = 0, \tag{5}$$

$$\left.\left(k\frac{\partial U_0}{\partial z} + h_0\left(U_0 - \Theta\right)\right)\right|_{z=h} = 0, \qquad \left.\left(k\frac{\partial U_1}{\partial z} + h_1\left(U_1 - \Theta\right)\right)\right|_{z=H} = 0, \tag{6}$$

$$\left.\left(-k\frac{\partial U_1}{\partial x} + h_1\left(U_1 - \Theta\right)\right)\right|_{x=l+0,\, z\in[h,H]} = 0; \tag{7}$$

where $\Theta = \Theta(t)$ is temperature of environment, but h_0, h_1 are heat convection coefficients for surfaces of corresponding sub-domains that also depend on temperature.

We also add conjugation conditions, i.e. continuity of the temperature and heat fluxes between both parts of the fuse:

$$U_0\big|_{x=l} = U_1\big|_{x=l}, \quad \left.\frac{\partial U_0}{\partial x}\right|_{x=l-0} = \left.\frac{\partial U_1}{\partial x}\right|_{x=l+0}, \qquad y \in [0,b],\ z \in [0,h]. \tag{8}$$

Finally, we add initial conditions:

$$U_0\big|_{t=0} = U_1\big|_{t=0} = U^0 = const \tag{9}$$

3.3 Conservative Averaging in *y*-direction

We introduce the integral average value of the functions $U_i(x, y, z, t)$ in the y-direction:

$$V_i(x,z,t) = \frac{1}{b}\int_0^b U_i(x,y,z,t)dy\,. \tag{10}$$

In praxis, firstly, the thickness b is very small in comparison with the width of the fuse. Secondly, the material of the fuse (metal) has high heat conductivity. These features allow us to use the simplest form of the conservative averaging method – approximation by a constant. The detailed procedure of the analytical transformations is given in Chapter 1. In short, we integrate the main equation (1) over the segment $y \in [0,b]$ and then we use boundary conditions (5) and linear representation of the source function (2). Finally, we take into account integral equality (10) and obtain differential equations with new functions $V_i(x,z,t)$:

$$\frac{\partial}{\partial t}\left(\gamma V_i\right) = \frac{\partial}{\partial x}\left(k\frac{\partial V_i}{\partial x}\right) + \frac{\partial}{\partial z}\left(k\frac{\partial V_i}{\partial z}\right) - \frac{h_i}{b}\left(V_i - \Theta\right) + F_i(V_i), \qquad i = \overline{0,1}. \tag{11}$$

Additional boundary conditions of new problem are the same as in the statement of the original problem (1)-(9):

$$\left.\frac{\partial V_0}{\partial x}\right|_{x=0} = \left.\frac{\partial V_1}{\partial x}\right|_{x=l+L} = 0, \quad \left.\frac{\partial V_i}{\partial z}\right|_{z=0} = 0, \quad i = \overline{0,1}, \tag{12}$$

$$\begin{gathered} \left.\left(k\frac{\partial V_0}{\partial z} + h_0\left(V_0 - \Theta\right)\right)\right|_{z=h} = 0, \\ \left.\left(k\frac{\partial V_1}{\partial z} + h_1\left(V_1 - \Theta\right)\right)\right|_{z=H} = 0, \end{gathered} \tag{13}$$

$$\left.\left(-k\frac{\partial V_1}{\partial x} + h_1\left(V_1 - \Theta\right)\right)\right|_{x=l+0,\, z\in[h,H]} = 0\,. \tag{14}$$

We add also conjugation conditions at $z \in [0,h]$:

$$V_0\big|_{x=l-0} = V_1\big|_{x=l+0}, \quad \left.\frac{\partial V_0}{\partial x}\right|_{x=l-0} = \left.\frac{\partial V_1}{\partial x}\right|_{x=l+0}; \tag{15}$$

and initial conditions:

$$V_0\big|_{t=0} = V_1\big|_{t=0} = U^0 = const\,. \tag{16}$$

3.4 Conservative Averaging in *x*-direction

As the next step, we will make conservative averaging in x-direction. We define one averaged value function over domain G_0 and two separate functions for the domain G_1 – the first for interval $z \in (0, h)$ and the second for interval $z \in (h, H)$ because of different conditions on the line $x = l$:

$$\begin{aligned}
&W_0(z,t) = \frac{1}{l}\int_0^l V_0(x,z,t)dx, \quad z \in (0,h),\\
&W_1(z,t) = \frac{1}{L}\int_l^{l+L} V_1(x,z,t)dx, \quad z \in (0,h),\\
&W_2(z,t) = \frac{1}{L}\int_l^{l+L} V_1(x,z,t)dx, \quad z \in (h,H).
\end{aligned} \tag{17}$$

In this case, we use exponential approximation in the following form:

$$V_0(x,z,t) = W_0(z,t) + p_0(z,t)\left[\cosh\left(\frac{x}{l}\right) - \sinh(1)\right], \tag{18}$$

$$V_1(x,z,t) = W_i(z,t) + p_i(z,t)\left[\cosh\left(\frac{x-l-L}{L}\right) - \sinh(1)\right], \quad i = \overline{1,2}\,. \tag{19}$$

Equalities (18), (19) are chosen in such a way that they fulfil integral equalities (17) (conservation of the heat energy) and boundary conditions (12) at $x = 0$ and $x = l + L$. We use conjugation conditions (15) to find unknown functions p_0 and p_1, and, afterwards, we obtain functions V_0, V_1:

$$V_0(x,z,t) = W_0(z,t) - C_0 l\big(W_0(z,t) - W_1(z,t)\big)\left[\cosh\left(\frac{x}{l}\right) - \sinh(1)\right], \tag{20}$$

$$V_1(x,z,t) = W_1(z,t) + C_0 L\big(W_0(z,t) - W_1(z,t)\big)\left[\cosh\left(\frac{x-l-L}{L}\right) - \sinh(1)\right], \tag{21}$$

$$C_0 = \frac{\mathrm{e}}{l+L}, \quad z \in (0,h)\,.$$

We find function p_2 and representation of the function V_1 in interval $z \in (h, H)$ from the expression (19) by means of the boundary condition (14):

$$V_1(x,z,t) = W_2(z,t) - C_1\big(W_2(z,t) - \Theta(t)\big)\left[\cosh\left(\frac{x-l-L}{L}\right) - \sinh(1)\right], \tag{22}$$

$$C_1 = \frac{2\,\mathrm{e}\,Lh_1}{k\left(\mathrm{e}^2 - 1\right) + 2Lh_1}, \quad z \in (h,H)\,.$$

Discontinuity for the temperature field could appear on the line $z = h$. This kind of discontinuities was considered also in paper [23].

We integrate differential equations (11) and we use representations (20), (21), (22) of the functions V_0, V_1 and integral equalities (17) to perform approximate analytical reduction of 2D system to 1D system of partial differential equations.

$$\frac{\partial}{\partial t}(\bar{\gamma}W_0) = \frac{\partial}{\partial z}\left(k\frac{\partial W_0}{\partial z}\right) + \frac{D_0}{l}\left(W_1 - W_0\right) - \frac{h_0}{b}\left(W_0 - \Theta\right) + F_0(W_0), \tag{23}$$

$$\frac{\partial}{\partial t}(\bar{\bar{\gamma}}W_1) = \frac{\partial}{\partial z}\left(k\frac{\partial W_1}{\partial z}\right) + \frac{D_0}{L}\left(W_0 - W_1\right) - \frac{h_1}{b}\left(W_1 - \Theta\right) + F_1(W_1), \tag{24}$$

$$\frac{\partial}{\partial t}(\bar{\bar{\bar{\gamma}}}W_2) = \frac{\partial}{\partial z}\left(k\frac{\partial W_2}{\partial z}\right) - D_1\left(W_2 - \Theta\right) - \frac{h_1}{b}\left(W_2 - \Theta\right) + F_1(W_2), \tag{25}$$

$$D_0 = C_0 k \sinh(1),\ D_1 = \frac{C_1 k \sinh(1)}{L^2}.$$

Again, boundary and initial conditions are the same as in the original problem:

$$\left.\frac{\partial W_0}{\partial z}\right|_{z=0} = 0,\ \left.\frac{\partial W_1}{\partial z}\right|_{z=0} = 0, \tag{26}$$

$$\begin{gathered}\left.\left(k\frac{\partial W_0}{\partial z} + h_0\left(W_0 - \Theta\right)\right)\right|_{z=h} = 0,\\ \left.\left(k\frac{\partial W_2}{\partial z} + h_1\left(W_2 - \Theta\right)\right)\right|_{z=H} = 0,\end{gathered} \tag{27}$$

$$\left.W_0\right|_{t=0} = \left.W_1\right|_{t=0} = \left.W_2\right|_{t=0} = U^0 = const. \tag{28}$$

We also ask for continuity of the averaged temperature and fluxes on the line $z = h$. That gives additional conjugation conditions:

$$\left.W_1\right|_{z=h-0} = \left.W_2\right|_{z=h+0},\ \left.\frac{\partial W_1}{\partial z}\right|_{z=h-0} = \left.\frac{\partial W_2}{\partial z}\right|_{z=h+0}. \tag{29}$$

An additional remark should be made about the current averaging step. As mentioned at the beginning of this chapter, we are considering a quasi-linear problem here. This situation significantly differs from the problems considered in Chapter 1 or in paper [24], where the averaging procedure was done over a sub-domain with a linear differential equation. Therefore, we will explain in a deeper way the averaging procedure for the left hand side of the equation (23) (the procedure can be accomplished for the equations (24) and (25) in the same way). Here, we use the *enthalpy* form of the heat equation (see, e.g. [35], Chapter 7). This form is substantially more suitable for the use of the mean value theorem:

$$\frac{1}{h}\int_0^h \frac{\partial}{\partial t}\left[\gamma(V_0)V_0\right]dz = \frac{\partial}{\partial t}\left[\gamma(\bar{V}_0)\frac{1}{h}\int_0^h V_0 dz\right] = \frac{\partial}{\partial t}\left[\bar{\gamma}W_0\right],$$

$$\bar{\gamma} = \gamma(\bar{V}_0),\ \bar{V}_0 = V_0\left(\bar{x}, z, t\right).$$

It is possible to choose mean value more or less freely. We propose to use corresponding middle point, i.e. $\bar{x} = l/2$, $\bar{\bar{x}} = \bar{\bar{\bar{x}}} = L/2$, or averaged temperature: $\bar{\gamma} = \gamma(W_0)$, $\bar{\bar{\gamma}} = \gamma(W_1)$, $\bar{\bar{\bar{\gamma}}} = \gamma(W_2)$. The latter is more convenient for calculations.

3.5 Conservative Averaging in z-direction

Finally, we will make conservative averaging procedure in z-direction. We introduce three new functions for this purpose:

$$u_0(t)=\frac{1}{h}\int_0^h W_0(z,t)dz,$$
$$u_1(t)=\frac{1}{h}\int_0^h W_1(z,t)dz, \tag{30}$$
$$u_2(t)=\frac{1}{H-h}\int_h^H W_2(z,t)dz.$$

We use exponential approximation in the form as follows:

$$W_0(z,t)=u_0(t)+q_0(t)\left[\cosh\left(\frac{z}{h}\right)-\sinh(1)\right],$$
$$W_1(z,t)=u_1(t)+q_1(t)\left[\cosh\left(\frac{z}{h}\right)-\sinh(1)\right], \tag{31}$$
$$W_2(z,t)=u_2(t)+q_2(t)\left[\cosh\left(\frac{z-h}{H-h}\right)-\sinh(1)\right]+$$
$$+q_3(t)\left[\sinh\left(\frac{z-h}{H-h}\right)-\cosh(1)+1\right].$$

We fulfil the integral equalities (conservation of the heat energy (30)) and the symmetry conditions (26) at $z=0$ by this representation. Using boundary conditions (27) and conjugation conditions (29), we can find four unknown parameters in the representation (31). This gives:

$$W_0(z,t)=u_0+e_0\left(u_0-\Theta\right)\left[\cosh\left(\frac{z}{h}\right)-\sinh(1)\right],$$
$$W_1(z,t)=u_1+\left[e_1\left(u_1-u_2\right)+e_2\left(u_2-\Theta\right)\right]\left[\cosh\left(\frac{z}{h}\right)-\sinh(1)\right], \tag{32}$$
$$W_2(z,t)=u_2+\left[e_3\left(u_1-u_2\right)+e_4\left(u_2-\Theta\right)\right]\left[\cosh\left(\frac{z-h}{H-h}\right)-\sinh(1)\right]+$$
$$+\left[e_5\left(u_1-u_2\right)+e_6\left(u_2-\Theta\right)\right]\left[\sinh\left(\frac{z-h}{H-h}\right)-\cosh(1)+1\right],$$
$$u_0=u_0(t),\quad u_1=u_1(t),\quad u_2=u_2(t);$$

where constants e_i are the following:

$$e_0=\frac{-2\,\mathrm{e}\,hh_0}{k(\mathrm{e}^2-1)+2hh_0},$$
$$e_1=-\mathrm{e}\,h\left(k(\mathrm{e}^2-1)+2h_1(H-h)\right)/e_7,$$
$$e_2=2\,\mathrm{e}\,hh_1(H-h)(\mathrm{e}^2-2\,\mathrm{e}-1)/e_7,$$

$$e_3 = (H-h)(\mathrm{e}^2-1)\left(k(\mathrm{e}^2+1)+2h_1(\mathrm{e}-1)(H-h)\right)/2e_7\,,$$
$$e_4 = -h_1(H-h)\left(2\,\mathrm{e}\,h+(\mathrm{e}^2-1)(\mathrm{e}-1)^2(H-h)\right)/e_7\,,$$
$$e_5 = -(H-h)(\mathrm{e}^2-1)\left(k(\mathrm{e}^2+1)+2h_1(\mathrm{e}-1)\right)/2e_7\,,$$
$$e_6 = h_1(H-h)^2(\mathrm{e}^2-1)(\mathrm{e}^2-2\,\mathrm{e}-1)/e_7\,,$$
$$e_7 = k(\mathrm{e}^2-1)(2H-h)+h_1(H-h)\left(2h-(\mathrm{e}^2-1)(\mathrm{e}-3)(\mathrm{e}-1)(H-h)\right).$$

Finally, we obtain system of ordinary differential equations after integration of equations (23)-(25):

$$\frac{d}{dt}(\tilde{\gamma}u_0) = \frac{D_0}{l}(u_1-u_0) - E_0(u_0-\Theta)+F_0(u_0), \tag{33}$$
$$\frac{d}{dt}(\tilde{\tilde{\gamma}}u_1) = \frac{D_0}{L}(u_0-u_1) - \frac{h_1}{b}(u_1-\Theta)+E_1\left[e_1(u_1-u_2)+e_2(u_2-\Theta)\right]+F_1(u_1), \tag{34}$$
$$\frac{d}{dt}(\hat{\gamma}u_2) = -E_2(u_1-u_2)-\left[E_3+D_1+\frac{h_y}{b}\right](u_2-\Theta)+F_1(u_2). \tag{35}$$

Here, constants E_0, E_1, E_2, E_3 and coefficients γ are as follows:

$$E_0 = \frac{h_0}{b}+\frac{h_0}{h}\left(1+\frac{e_0}{\mathrm{e}}\right), \quad E_1 = \frac{k\sinh(1)}{h^2}, \quad E_2 = \frac{k\left(e_3\sinh(1)+e_5(\cosh(1)-1)\right)}{(H-h)^2},$$
$$E_3 = \frac{k\left(e_4\sinh(1)+e_6(\cosh(1)-1)\right)}{(H-h)^2},$$
$$\tilde{\gamma} = \overline{\gamma}\left(W_0(\tilde{z},t)\right),\ \tilde{\tilde{\gamma}} = \overline{\overline{\gamma}}\left(W_1(\tilde{z},t)\right),\ \hat{\gamma} = \overline{\overline{\overline{\gamma}}}\left(W_1(\hat{z},t)\right),\ \tilde{z}=h/2,\ \hat{z}=(H+h)/2;$$
$$\text{or } \tilde{\gamma} = \overline{\gamma}\left(u_0(t)\right),\ \tilde{\tilde{\gamma}} = \overline{\overline{\gamma}}\left(u_1(t)\right),\ \hat{\gamma} = \overline{\overline{\overline{\gamma}}}\left(u_2(t)\right),$$

This zero-space-dimensional (0D) system of three ordinary differential equations must be supplemented with initial conditions:

$$u_0\big|_{t=0} = u_1\big|_{t=0} = U^0. \tag{36}$$

3.6 Simplified Averaged System of Ordinary Differential Equations

The main goal of this mathematical model is to predict the time before the melting of the material in the thinnest sub-domain G_0 caused by an unwithstandably strong current. According to the expression (2), the density of the electric current is H^2/h^2 times larger in this sub-domain. This allows us to propose another model besides the first one. As the second step of the averaging, we use the simplest approximation in the *z*-direction – approximation by constant.

We introduce averaged values:

$$\begin{aligned} w_0(x,t) &= \frac{1}{h}\int_0^h V_0(x,z,t)\,dz, \\ w_1(x,t) &= \frac{1}{H}\int_0^H V_1(x,z,t)\,dz; \end{aligned} \tag{37}$$

and assume that temperature is constant in z-direction because it changes only slightly in comparison with x-direction:

$$\begin{aligned} w_0(x,t) &= V_0(x,z,t), \\ w_1(x,t) &= V_1(x,z,t). \end{aligned} \tag{38}$$

Integration of the differential equations (11) immediately gives system of two 1D partial differential equations:

$$\begin{aligned} \frac{\partial}{\partial t}\big(\gamma(w_0)w_0\big) &= \frac{\partial}{\partial x}\left(k\frac{\partial w_0}{\partial x}\right) - h_0\left(\frac{1}{b}+\frac{1}{h}\right)\big(w_0-\Theta\big) + F_0(w_0), \\ \frac{\partial}{\partial t}\big(\gamma(w_1)w_1\big) &= \frac{\partial}{\partial x}\left(k\frac{\partial w_1}{\partial x}\right) - h_1\left(\frac{1}{b}+\frac{1}{H}\right)\big(w_1-\Theta\big) + F_1(w_1). \end{aligned} \tag{39}$$

Boundary conditions remain the same:

$$\left.\frac{\partial w_0}{\partial x}\right|_{x=0} = \left.\frac{\partial w_1}{\partial x}\right|_{x=l+L} = 0. \tag{40}$$

The second conjugation condition changes substantially because of convective heat losses over the surface $\{x = l, z \in [h, h+H]\}$:

$$\begin{aligned} &w_0\big|_{x=l-0} = w_1\big|_{x=l+0}, \\ &hk\left.\frac{\partial w_0}{\partial x}\right|_{x=l-0} = \left.\left[Hk\frac{\partial w_1}{\partial x} - h_1\big(H-h\big)\big(w_1-\Theta\big)\right]\right|_{x=l+0}. \end{aligned} \tag{41}$$

Integration of the boundary condition and conjugation conditions was made to obtain previous equation. Such type of the second conjugation condition was used also in paper [34]. The initial conditions remain the same:

$$w_0\big|_{t=0} = w_1\big|_{t=0} = U^0. \tag{42}$$

As the last step, we apply the conservative averaging method in x-direction. We use exponential approximation in the form used earlier:

$$\begin{aligned} w_0(x,t) &= u_0(t) + p_0(t)\left[\cosh\left(\frac{x}{l}\right) - \sinh\big(1\big)\right], \\ w_1(x,t) &= u_1(t) + p_1(t)\left[\cosh\left(\frac{x-l-L}{L}\right) - \sinh\big(1\big)\right]. \end{aligned} \tag{43}$$

We have introduced the average integral values again:

$$\begin{aligned} u_0(t) &= \frac{1}{l}\int_0^l w_0(x,t)dx, \\ u_1(t) &= \frac{1}{L}\int_l^{l+L} w_1(x,t)dx. \end{aligned} \tag{44}$$

We obtain parameters $p_0(t)$ and $p_1(t)$ of the representations (43) out of the conjugation conditions (41):

$$p_0(t) = e\frac{g_1\big(u_1-u_0\big) - g_2\big(u_0-\Theta\big)}{g_3}, \quad p_1(t) = e\frac{g_0\big(u_0-u_1\big) - g_2\big(u_1-\Theta\big)}{g_3}.$$

Here, $g_0 = k\dfrac{h}{l}\left(e^2-1\right)$, $g_1 = k\dfrac{H}{L}\left(e^2-1\right)$, $g_2 = 2h_1\left(H-h\right)$, $g_3 = g_0+g_1+g_2$.

Finally, we integrate partial differential equations (39) and obtain system of ordinary differential equations:

$$\frac{d}{dt}\left(\bar{\gamma}u_0\right) = \frac{G}{l^2}\left[\left(g_1+g_2\right)\left(u_1-u_0\right)-g_2\left(u_1-\Theta\right)\right]-h_0\left(\frac{1}{b}+\frac{1}{h}\right)\left(u_0-\Theta\right)+F_0(u_0), \quad (45)$$

$$\frac{d}{dt}\left(\bar{\bar{\gamma}}u_1\right) = \frac{G}{L^2}\left[g_0\left(u_0-u_1\right)-g_2\left(u_1-\Theta\right)\right]-h_1\left(\frac{1}{b}+\frac{1}{H}\right)\left(u_1-\Theta\right)+F_1(u_1); \quad (46)$$

where $\bar{\gamma} = \gamma\left(w_0(\bar{x},t)\right)$ or $\bar{\gamma} = \gamma\left(u_0(t)\right)$, $\bar{x} = l/2$,

$\bar{\bar{\gamma}} = \gamma\left(w_1(\bar{\bar{x}},t)\right)$ or $\bar{\bar{\gamma}} = \gamma\left(u_1(t)\right)$, $\bar{x} = l/2$,

$$G = \frac{k\left(e^2-1\right)}{2g_3}.$$

It remains to add the initial conditions for the completeness of the full statement of the 0D problem:

$$u_0\big|_{t=0} = u_1\big|_{t=0} = U^0. \quad (47)$$

3.7 Numerical Example of 50A Fuse

An automotive fuse of the nominal current $I_0 = 50\text{A}$ (Fig. 3.6) is taken as a sample. Geometry is transferred to our mathematical model (Fig. 3.5). One eighth of the fuse is considered because of the symmetry. Notations of the dimensions are as before in this chapter: $l = 13mm$, $L = 27mm$, $b = 0.2mm$, $h = 1.9mm$, $H = 8mm$. Dimensions are obtained by measuring the fuse.

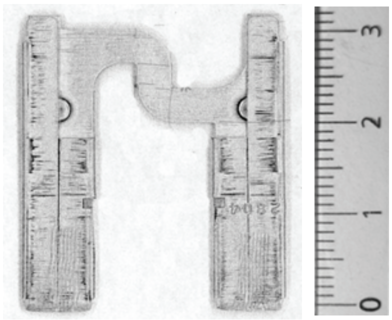

Fig. 3.6: 50A fuse without shell

Fuse is made of zinc. Properties of the material depend on temperature. Values are known at some reference temperatures [26], and spline is constructed from them. It is satisfactory to use linear spline (Fig. 3.7, Fig. 3.8).

Fig. 3.9 shows heat convection coefficient h_0 and h_1. Solid line is for the thinnest part of the fuse $x \in (0,l)$; dash line is for the interval $x \in (l,L)$. Temperature of environment is 65°C.

Next figures show how much heat is produced by electric current in the thinner part of the fuse F_0 (Fig. 3.10) and in the blades F_1 (Fig. 3.11) at different current values.

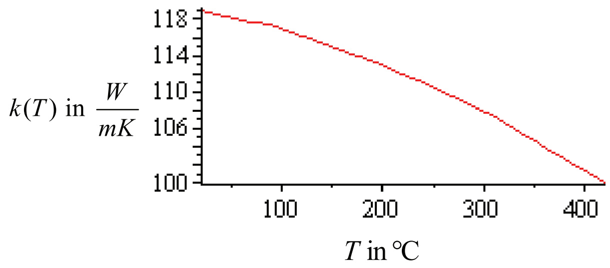

Fig. 3.7: Heat conductivity of zinc

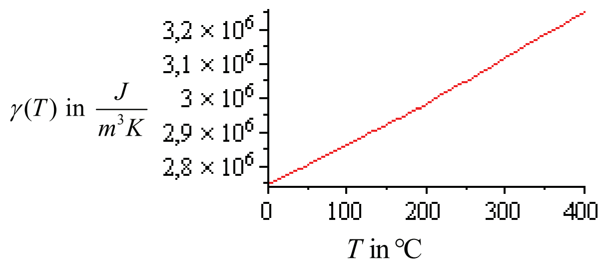

Fig. 3.8: Volumetric heat capacity of zinc

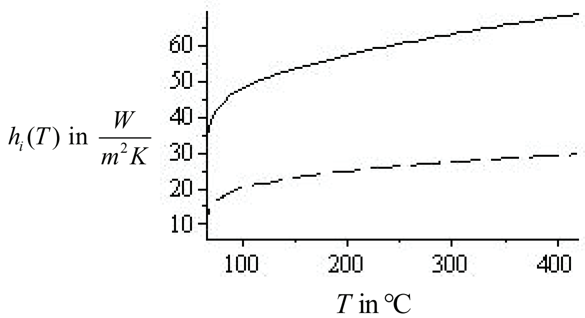

Fig. 3.9: Heat convection to air

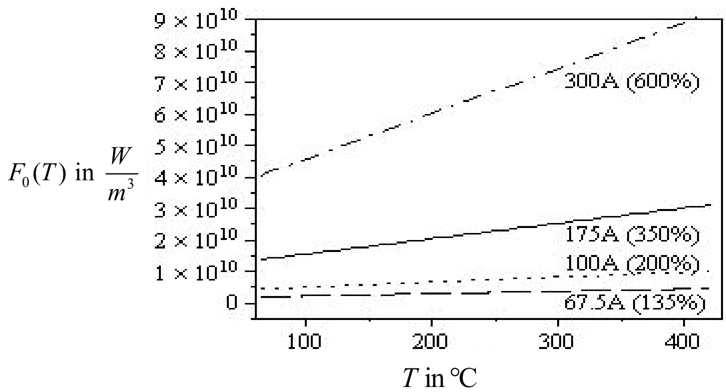

Fig. 3.10: Heat release-rate F_0 in the thinner part of the fuse

It is visible from the figures that heat production in the thinner part is more than 10 times larger than in the other part of the fuse.

Numerical calculations are done in 3 different ways. First, solution is obtained from the system of 3 ODE-s (33)-(35). Second, calculations are done from the system of 2 ODE-s (45)-(46). Third, 1D mathematical problem that consists of PDE-s (39) and

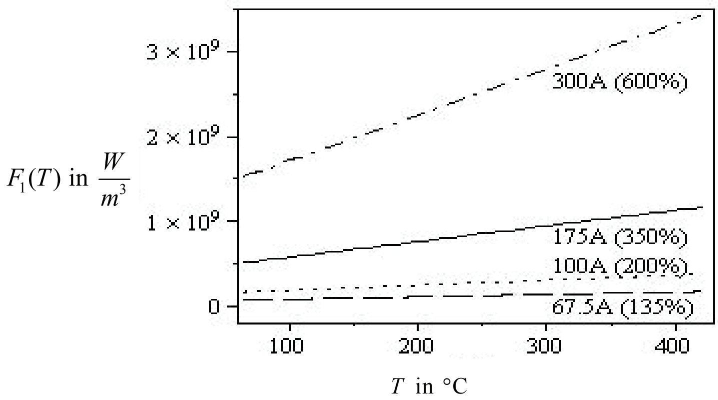

Fig. 3.11: Heat release-rate F_1 in the blades of the fuse

additional conditions (40)-(42) is solved by applying finite difference method together with factorization method. Results are compared altogether and with the standard DIN 72581-3 that define time interval of the burn-out of fuses (Table 3.1).

I / I_0	Min.	Max.
600 %	0.04 s	1 s
350 %	0.2 s	7 s
200 %	2 s	60 s
135 %	60 s	1800 s

Table 3.1: Burn-out interval of fuses defined by the standard DIN 72581-3

Maximal temperature is reached in the middle of the fuse. Time to reach melting temperature is calculated and compared among all three mathematical models (Table 3.2, Fig. 3.12). Dash lines are time limits from the DIN standard.

I / I_0	1D PDE-s	3 ODE-s	2 ODE-s
600 %	0.25 s	0.24 s	0.24 s
350 %	0.78 s	0.74 s	0.76 s
200 %	3.4 s	2.9 s	3.7 s
135 %	19 s	11.6 s	23 s

Table 3.2: Time to reach the melting temperature

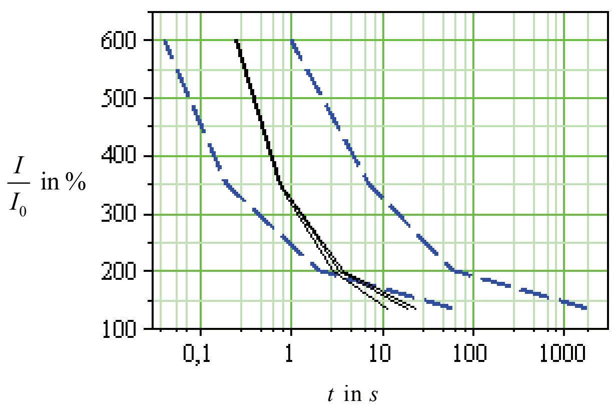

Fig. 3.12: Time-current curve of a 50A fuse

Numerical results are appropriate if current is greater than 200% of the rating. Heat conduction through the blades, which is not considered in this particular model, plays a greater role only if current is close to the nominal value. This is the reason why the curve inclines to the left at the bottom of the figure – the real fuse breaking time is larger. This and also the heat radiation of a surface could be added to the original 3D mathematical model. Conservative averaging could be applied in the same manner.

For example, if we take into account heat radiation, additional term should be added to the boundary conditions (5)-(7):

$$\left.\left(k\frac{\partial U_i}{\partial y}+h_i\left(U_i-\Theta\right)+\varepsilon\sigma\left(U_i^4-\Theta^4\right)\right)\right|_{y=b}=0, \tag{48}$$

$$\left.\left(k\frac{\partial U_0}{\partial z}+h_0\left(U_0-\Theta\right)+\varepsilon\sigma\left(U_0^4-\Theta^4\right)\right)\right|_{z=h}=0,$$
$$\left.\left(k\frac{\partial U_1}{\partial z}+h_1\left(U_1-\Theta\right)+\varepsilon\sigma\left(U_1^4-\Theta^4\right)\right)\right|_{z=H}=0, \tag{49}$$

$$\left.\left(-k\frac{\partial U_1}{\partial x}+h_1\left(U_1-\Theta\right)+\varepsilon\sigma\left(U_i^4-\Theta^4\right)\right)\right|_{x=l+0,z\in[h,H]}=0. \tag{50}$$

3D temperature distribution could be reconstructed whomever averaging is chosen. It is enough to show temperature only in (x,z) plane because we have assumption about constant temperature distribution over y-dimension. Fig. 3.13 shows temperature reconstruction in the fuse when the melting point is reached after system of 2 ODE-s is solved in the case of 100A (200%) electric current.

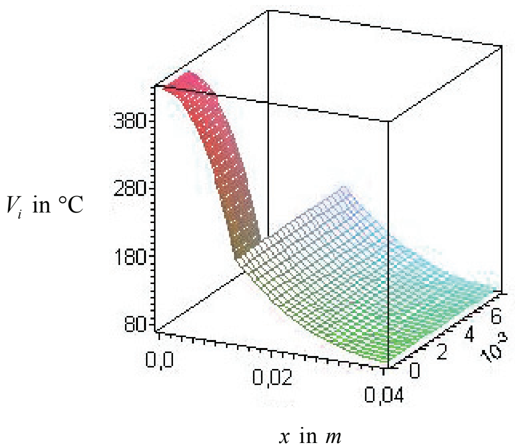

Fig. 3.13: Temperature distribution. 100A current (200%). 2 ODE-s model

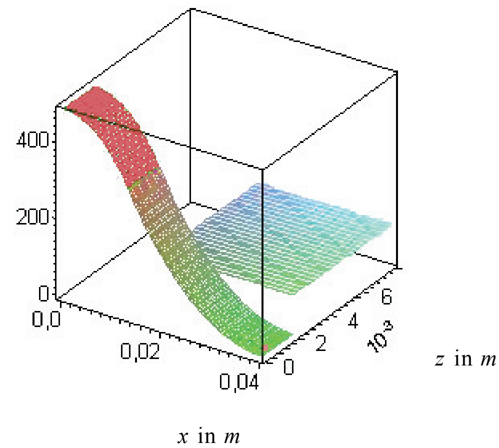

Fig. 3.14: Temperature distribution. 100A current (200%). 3 ODE-s model

Similar graphic (Fig. 3.14) could be obtained for the solution of 3 ODE-s by formulae (20)-(22), (31). Solution is discontinuous because discontinuous approximation function $V_1(x,z,t)$ was used ((21)-(22)).

Solution of 1D PDE-s should be used if temperature distribution in the fuse is also important and not only fuse breaking time. Fig. 3.15 shows temperature on the line $x\in[0,L]$.

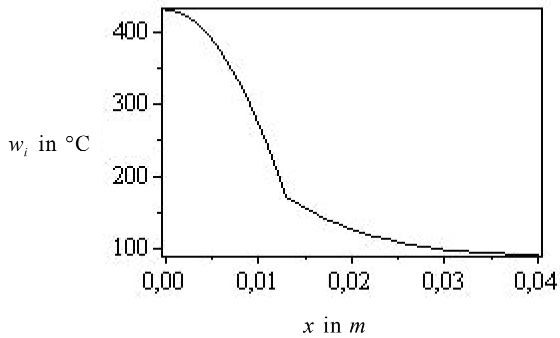

Fig. 3.15: Temperature distribution on x axis. 100A current (200%). 1D PDE-s model

Next figure (Fig. 3.16) contains temperature distribution on the line $x \in [0, L]$ for all mathematical models used.

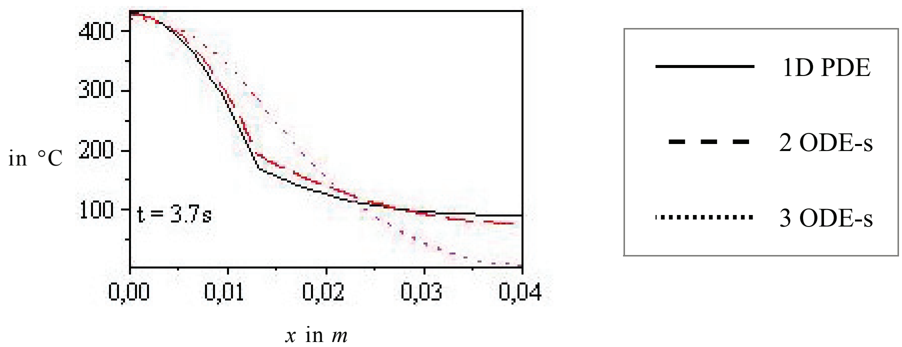

Fig. 3.16: Temperature distribution on x-axis. All models compared

It takes about one minute on modern desktop computer to calculate particular example at given current. Calculation of ODE-s is even quicker. It is more efficient to calculate averaged mathematical problems rather than full 3D problems.

3.8 Conclusions

We have approximated a 3D problem and reduced its solution to the solution of the time-dependent non-linear system of two or three ordinary differential equations. Reduction was realized in two different ways by different assumptions. Both systems have a similar structure, but different coefficients. To keep higher calculation precision for temperature distribution in a fuse, a 1D PDE model could be used. The systems of differential equations developed are solvable with standard techniques and in a short time. An approximate analytical 3D solution could easily be obtained from the solution of the transformed problem afterwards.

4 Cylindrical Model of Automotive Fuse

Continuation of the research on automotive fuses led to new mathematical models that are described in this chapter. Geometry of a fuse is represented by cylindrical bodies in this case. As before, 3D problem is stated and then altered by conservative averaging method.

Although, every proper fuse brakes at short circuit, problem with heat up rises when current is around nominal. Fuse generates extra heat that goes into wires and quicker degrades insulation if current is close to nominal or slightly above. Improved models take into account heat generation and conduction in wires that are connected to fuse.

4.1 Geometry of the Model

The same type of fuses as in the previous chapter are considered (Fig. 3.1, Fig. 3.2). We straighten out the fuse and use the geometry of the model as shown in Fig. 4.1 (half is used because of the symmetry in the middle). Sub-domain 1 represents the thinnest part of the fuse – the “fuse element”. The second part we shall call the “fuse socket”. This consists of fuse blades and the fuse box. Sub-domain 3 is the wire that is connected to the fuse (Fig. 4.2).

In reality, the geometry of the fuse socket is not the same for every car model. That makes it difficult to make universal calculations even for specific fuse. The goal is to find rules which would make fuse design easier and fuse behaviour more stable and predictable.

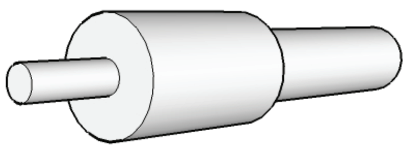

Fig. 4.1: Geometry of the model in 3D

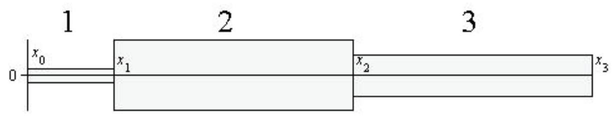

Fig. 4.2: Geometry of the model

Besides geometry, this model takes into account connected wire (sub-domain 3) and heat radiation in comparison with the parallelepiped model in the Cartesian coordinate system presented in Chapter 3.

4.2 Original Problem and its Approximation by Conservative Averaging Method

4.2.1 Mathematical Statement of Full Problem

We continue with formulation of three-dimensional mathematical model of the transient heat conduction in a fuse body. As in previous chapter, count of dimensions corresponds to the space dimensions.

Let us treat main domain (Fig. 4.2) as three connected sub-domains G_1, G_2 and G_3:

$$G_i = \{(x,r,\varphi) \mid x \in [x_{i-1}, x_i], r \in [0, r_i], \varphi \in [0, 2\pi]\}, \quad i = \overline{1,3}.$$

Index i indicate corresponding sub-domain throughout the text.

Temperature distribution does not depend on angle φ; and we have two space dimensions to consider. If temperature in domain G_i is denoted as function $U_i(x,r,t)$, differential equation for heat transfer is as follows:

$$\frac{\partial}{\partial t}(\gamma_i U_i) = \frac{\partial}{\partial x}\left(k_i \frac{\partial U_i}{\partial x}\right) + \frac{1}{r}\frac{\partial}{\partial r}\left(r k_i \frac{\partial U_i}{\partial r}\right) + F_i(U_i), \tag{1}$$

$$(x,r) \in G_i, \quad t > 0, \quad i = \overline{1,3}.$$

Heat conductivity $k_i(U_i)$ and volumetric heat capacity $\gamma_i(U_i)$ depend on temperature. Source function F_i represents heat produced by electric current. It is approximated by linear function:

$$F_i(U_i) = B_i\left(1 + \alpha_{r,i}\left(U_i - U_r\right)\right), \quad B_i = \frac{I^2 \rho_{ref,i}}{\pi^2 r_i^4}. \tag{2}$$

Parameter $\rho_{ref,i}$ is resistivity of the material at the reference temperature U_r; $\alpha_{r,i}$ is temperature coefficient of electric resistivity; I – electric current.

Besides main equations (1), we add symmetry (no flux) conditions on x axis and at the endings of the model:

$$\left.\frac{\partial U_i}{\partial r}\right|_{r=0} = 0; \tag{3}$$

$$\left.\frac{\partial U_1}{\partial x}\right|_{x=0} = 0, \tag{4}$$

$$\left.\frac{\partial U_3}{\partial x}\right|_{x=x_3} = 0. \tag{5}$$

It is acceptable to assume that there is no heat flux also on the free parts of the joining surfaces of the cylinders:

$$\left.\frac{\partial U_2}{\partial x}\right|_{x=x_1, r\in[r_1,r_2]} = 0, \quad \left.\frac{\partial U_2}{\partial x}\right|_{x=x_2, r\in[r_2,r_3]} = 0. \tag{6}$$

We also add heat exchange conditions on the outer surfaces in r-direction:

$$\left.\left(k_i \frac{\partial U_i}{\partial r} + \alpha_i\left(U_i - \Theta_i\right)\right)\right|_{r=r_1} = 0, \tag{7}$$

where α_i is non-linear heat exchange coefficient that depend on temperature; Θ_i is ambient temperature that could be different for each sub-domain of the model. Coefficient α_i is the sum of two components:

$$\alpha = \alpha_{conv} + \alpha_{rad}.$$

Convection coefficient α_{conv} is usually obtained from reference books e.g. [26], [36]. Heat radiation coefficient α_{rad} comes from Stefan–Boltzmann law:

$$\alpha_{rad} = \varepsilon\sigma\left(U_i^2 + \Theta_i^2\right)\left(U_i + \Theta_i\right).$$

Conjugation conditions are added to the statement of the mathematical problem, i.e. continuity of the temperature and heat fluxes between cylinders:

a) $x = x_1, r \in [0, r_1]$:

$$U_1\Big|_{x=x_1} = U_2\Big|_{x=x_1}, \tag{8}$$

$$k_1 \frac{\partial U_1}{\partial x}\bigg|_{x=x_1-0} = k_2 \frac{\partial U_2}{\partial x}\bigg|_{x=x_1+0}; \tag{9}$$

b) $x = x_2, r \in [0, r_3]$:

$$U_2\Big|_{x=x_2} = U_3\Big|_{x=x_2}, \tag{10}$$

$$k_2 \frac{\partial U_2}{\partial x}\bigg|_{x=x_2-0} = k_3 \frac{\partial U_3}{\partial x}\bigg|_{x=x_2+0}. \tag{11}$$

Finally, we add initial conditions:

$$U_i\Big|_{t=0} = U^0 = const. \tag{12}$$

4.2.2 Conservative Averaging in *r*-direction

We introduce the integral average value of the function $U_i(x,r,t)$ over the radius r:

$$V_i(x,t) = \frac{2}{r_i^2}\int_0^{r_i} rU_i(x,r,t)dr. \tag{13}$$

General description of conservative averaging in polar coordinates is given in Chapter 1.3.

Temperature gradients in r-direction are very small in comparison with x-direction. This allows us to use the simplest form of the conservative averaging method – approximation by the constant:

$$V_i(x,t) = U_i(x,r,t). \tag{14}$$

Next, we apply the same integral as in formula (13) to the differential equation (1):

$$\frac{2}{r_i^2}\int_0^{r_i} \frac{\partial}{\partial t}\left(\gamma_i U_i\right) dr = \frac{2}{r_i^2}\int_0^{r_i}\left[\frac{\partial}{\partial x}\left(k_i \frac{\partial U_i}{\partial x}\right) + \frac{1}{r}\frac{\partial}{\partial r}\left(rk_i \frac{\partial U_i}{\partial r}\right) + F_i(U_i)\right]dr.$$

We change the order of the integration and differentiation and take into account integral (13) to substitute function U_i by V_i:

$$\frac{\partial}{\partial t}\left(\gamma_i V_i\right) = \frac{\partial}{\partial x}\left(k_i \frac{\partial V_i}{\partial x}\right) + \frac{2}{r_i^2} rk_i \frac{\partial U_i}{\partial r}\bigg|_0^{r_i} + F_i(V_i).$$

Source function is the same because of its linear representation (2). We use boundary conditions (3) and (7) to substitute derivatives of r and obtain new partial differential equation of averaged function $V_i(x,t)$:

$$\frac{\partial}{\partial t}\left(\gamma_i V_i\right) = \frac{\partial}{\partial x}\left(k_i \frac{\partial V_i}{\partial x}\right) - \frac{2}{r_i}\alpha_i\left(V_i - \Theta_i\right) + F_i(V_i). \tag{15}$$

It has one dimension less than in original problem (1). Coefficients are calculated from averaged values because of constant approximation (14):

$$k_i = k_i(V_i),\ \gamma_i = \gamma_i(V_i) \text{ and } \alpha_i = \alpha_i(V_i).$$

We need to add also conjugation conditions between cylinders. First, we ask for temperature continuity:

$$V_1\big|_{x=x_1} = V_2\big|_{x=x_1}, \tag{16}$$

$$V_2\big|_{x=x_2} = V_3\big|_{x=x_2}. \tag{17}$$

Second, we ascertain that heat power is the same on both sides of connection point:

$$r_1^2 k_1 \frac{\partial V_1}{\partial x}\bigg|_{x=x_1} = r_2^2 k_2 \frac{\partial V_2}{\partial x}\bigg|_{x=x_1} \tag{18}$$

$$r_2^2 k_2 \frac{\partial V_2}{\partial x}\bigg|_{x=x_2} = r_3^2 k_3 \frac{\partial V_3}{\partial x}\bigg|_{x=x_2} \tag{19}$$

Remaining boundary and initial conditions of new problem are similar as in the statement of the original problem (1)-(12):

$$\frac{\partial V_1}{\partial x}\bigg|_{x=0} = 0, \tag{20}$$

$$\frac{\partial V_3}{\partial x}\bigg|_{x=x_3} = 0, \tag{21}$$

$$V_i\big|_{t=0} = U^0 = const. \tag{22}$$

Instead of (1)-(12), we obtained new mathematical problem (15)-(22) that has one space dimension less. Solution could be calculated by numerical methods. Description of building finite differences for such mathematical problem is given in Appendix 1.

4.2.3 Conservative Averaging in *x*-direction

As the next step, we will make conservative averaging in *x*-direction. We define averaged value functions over each domain G_i:

$$u_i(t) = \frac{1}{l_i}\int_0^{l_i} V_i(x,t)\,dx. \tag{23}$$

Here, we will use exponential approximation over *x* in the following form:

$$\begin{aligned} V_i(x,t) = u_i(t) + p_i(t)\left[\cosh\left(\frac{x-x_{i-1}}{l_i}\right) - \sinh(1)\right] + \\ +q_i(t)\left[\sinh\left(\frac{x-x_{i-1}}{l_i}\right) - \cosh(1) + 1\right],\quad l_i = x_i - x_{i-1},\ i = \overline{1,3}. \end{aligned} \tag{24}$$

Equalities (24) are chosen in such a way that they fulfil integral (23) (conservation of heat energy). We obtain system of six equations from boundary and conjugation conditions (16)-(21):

$$u_1 + p_1 \mathrm{e}^{-1} = u_2 + p_2\left(1 - \sinh(1)\right) + q_2\left(1 - \cosh(1)\right),$$

$$u_2 + p_2\,\mathrm{e}^{-1} + q_2\left(1-\mathrm{e}^{-1}\right) = u_3 + p_3\left(1-\sinh(1)\right) + q_3\left(1-\cosh(1)\right),$$
$$r_1^2\bar{k}_1 l_1^{-1}\sinh(1)\,p_1 = r_2^2\bar{k}_2 l_2^{-1} q_2,$$
$$r_2^2\bar{\bar{k}}_2 l_2^{-1}\left(\sinh(1)\,p_2 + \cosh(1) q_2\right) = r_3^2\bar{k}_3 l_3^{-1} q_3,$$
$$\sinh(1)\,p_3 + \cosh(1) q_3 = 0,$$
$$q_1 = 0;$$

where coefficients are as follows:

$$\bar{k}_1 = k(V_1(x_1,t)),\quad \bar{k}_2 = k(V_2(x_1,t)),\quad \bar{\bar{k}}_2 = k(V_2(x_2,t)),\quad \bar{k}_3 = k(V_3(x_2,t)).$$

Functions V_1, V_2, V_3 are determined by solving the system and finding unknown functions p_i, q_i:

$$q_2(t) = \left[\left(\sinh(1)-1\right)\left(u_2(t)-u_3(t)\right) - \frac{1+G_{23}}{\mathrm{e}}\left(u_1(t)-u_2(t)\right)\right]$$
$$\Bigg/\left[\frac{(1+G_{23})}{\mathrm{e}}\left(\frac{G_{21}}{\mathrm{e}\sinh(1)} + \cosh(1) - 1\right) - \left(\sinh(1)-1\right)\left(\frac{G_{23}}{\mathrm{e}\tanh(1)} + 1 - \frac{1}{\mathrm{e}}\right)\right],$$
$$p_2(t) = \frac{-q_2(t)}{\sinh(1)-1}\left(\frac{G_{21}}{\mathrm{e}\sinh(1)} + \cosh(1) - 1\right) - \frac{u_1(t)-u_2(t)}{\sinh(1)-1},$$
$$q_3(t) = G_{23}\left(p_2(t)\sinh(1) + q_2(t)\cosh(1)\right),$$
$$p_3(t) = q_3(t)/\tanh(1),$$
$$p_1(t) = q_2(t) G_{21}/\sinh(1);$$

where $G_{21} = \dfrac{r_2^2\bar{k}_2 l_1}{r_1^2\bar{k}_1 l_2}$, $G_{23} = \dfrac{r_2^2\bar{\bar{k}}_2 l_3}{r_3^2\bar{k}_3 l_2}$.

Next, we integrate differential equations (15):

$$\int_{x_{i-1}}^{x_i}\frac{\partial}{\partial t}\left(\gamma_i V_i\right)dx = \int_{x_{i-1}}^{x_i}\left[\frac{\partial}{\partial x}\left(k_i\frac{\partial V_i}{\partial x}\right) - \frac{2}{r_i}\alpha_i\left(V_i-\Theta_i\right) + F_i(V_i)\right]dx.$$

We use representations (24) of the functions V_i and integral equalities (23) to make approximate analytical reduction of 1D system to the system of three ordinary differential equations:

$$\frac{d}{dt}(\bar{\gamma}_1 u_1) = p_1\frac{\bar{k}_1\sinh(1)}{l_1^2} - \frac{2}{r_1}\bar{\alpha}_1\left(u_1-\Theta_1\right) + F_1(u_1), \tag{25}$$

$$\frac{d}{dt}(\bar{\gamma}_2 u_2) = p_2\frac{\bar{\bar{k}}_2\sinh(1)}{l_2^2} + q_2\frac{+\bar{\bar{k}}_2\cosh(1) - \bar{k}_2}{l_2^2} - \frac{2}{r_2}\bar{\alpha}_2\left(u_2-\Theta_2\right) + F_2(u_2), \tag{26}$$

$$\frac{d}{dt}(\bar{\gamma}_3 u_3) = -\frac{\bar{k}_3}{l_3^2}q_3 - \frac{2}{r_3}\bar{\alpha}_3\left(u_3-\Theta_3\right) + F_3(u_3). \tag{27}$$

Coefficients $\bar{\gamma}_i$ and $\bar{\alpha}_i$ are mean values of γ_i and α_i. In general, it is not possible to determine them analytically. We propose to use averaged temperature for calculations:

$$\bar{\gamma}_i(t) = \gamma(u_i(t)),\quad \bar{\alpha}_i(t) = \alpha_i(u_i(t)),\quad i = \overline{1,3}.$$

It remains to add an initial condition to complete the 0D mathematical statement:

$$u_i\big|_{t=0} = U^0 = const\,. \tag{28}$$

After solving (25)-(28), approximated solution of the original problem could be obtained by formulae (14) and (24).

4.3 Comparison of Finite Element and Conservative Averaging Methods

We will compare numerical results of original 3D model and two simplified models from previous chapter: (15)-(22) and (25)-(28). Finite elements approach is used to calculate temperatures in 3D model. For 1D PDE-s, finite difference method is used.

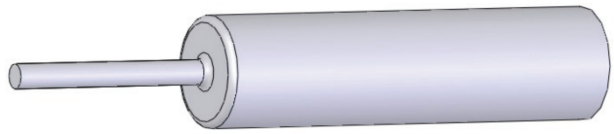

Fig. 4.3: 3D model of the example

Let us take the following parameters as an example (Fig. 4.3):

$$r_1 = 0.355mm,\ r_2 = r_3 = 1.6mm,\ l_i = 6mm,\ \varepsilon_1 = 0.07,\ \varepsilon_2 = \varepsilon_3 = 0.93,$$

$$\rho_{ref,i} = 1.045\cdot 10^{-7}\,\Omega m,\ \alpha_{ref,i} = 0,\ \Theta_i = 65^\circ C,\ i = \overline{1,3};$$

and the temperature dependant coefficients k, γ of zinc [26]. A fixed value is used for the resistivity. The melting temperature of zinc is 419.5°C. Simplified fuse geometry is used but not a concrete existing sample.

The maximum temperature is reached in the middle of the fuse. Time to reach the melting temperature at a given electric current is calculated and compared among all three mathematical models (Table 4.1, Fig. 4.4).

Current	3D model	1D PDE-s	ODE-s
180A	0.050s	0.056s	0.040s
105A	0.15s	0.18s	0.14s
60A	0.84s	1.0s	1.3s
40.5A	21s	25s	27s

Table 4.1: Time to reach melting point at given current

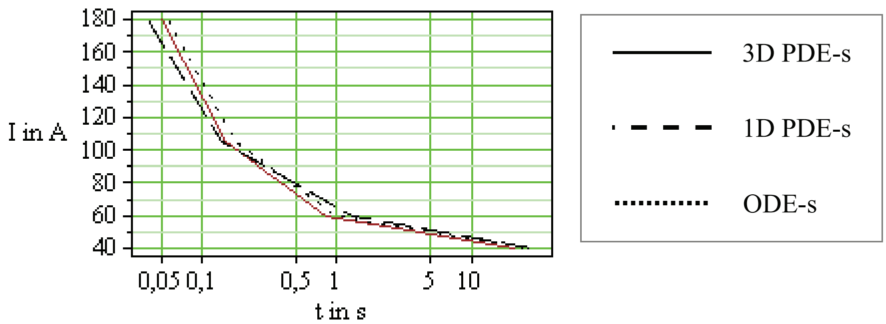

Fig. 4.4: Time-current curve

Distribution of temperature on x axis is shown in Fig. 4.5 – Fig. 4.8 at time moment when 3D model reaches melting point.

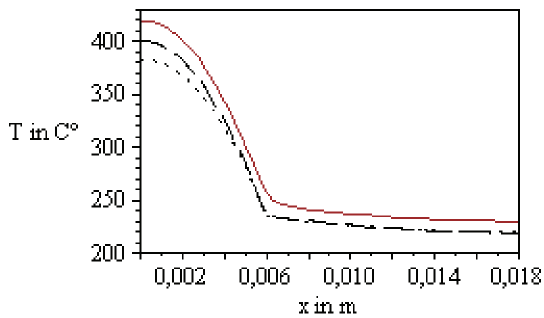

Fig. 4.5: Temperature at 40.5A current

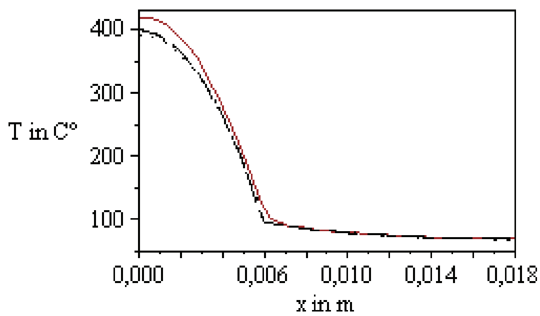

Fig. 4.6: Temperature at 60A current

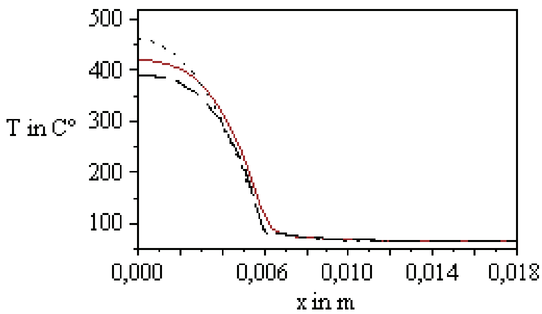

Fig. 4.7: Temperature at 105A current

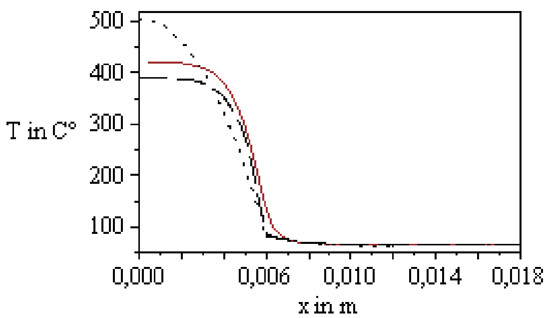

Fig. 4.8: Temperature at 180A current

It is visible from curve (Fig. 4.4) that 0D model is sufficient to determine time-current characteristics of the fuse. Solution of the 1D PDE-s should be used if temperature distribution in the fuse is also important and not only fuse breaking time.

4.4 Numerical Example of 25A Fuse

An automotive fuse of the nominal current $I_0 = 25\text{A}$ is taken as a sample (Fig. 4.9).

Fig. 4.9: 25A fuse

The geometry is transferred to our mathematical model (Fig. 4.2). We assume that wires of cross-section $2.4mm^2$ are connected to the fuse. Dimensions are obtained by measuring the fuse:

$$r_1 = 0.38mm,\ r_2 = 1.1mm\ \ r_3 = 0.87mm,\ l_1 = 5.7mm,\ l_2 = 17mm,\ l_3 = 20mm,$$

$$\Theta_i = 65^\circ C,\ i = \overline{1,3},\ \varepsilon_1 = 0.07,\ \varepsilon_2 = \varepsilon_3 = 0.93.$$

The fuse is made of zinc, and the wire – of a copper alloy called CuETP. Properties of these materials (heat conductivity and capacity) depend on temperature [26].

The dimensions of the insulation of the wires and the fuse socket are taken into account when calculating heat convection coefficient α_{conv}. Outer radius of the wire is 1.4mm; for fuse socket – 2.1mm. Computation of the coefficient α_{conv} was done as suggested in [16].

1D mathematical model (15)-(22) was taken for numerical calculations of this fuse. Results are compared with standard DIN 72581-3 that define time interval of the burn-out of the fuses of this type (Table 4.2, Fig. 4.10). Dash lines are time limits of DIN standard.

% of Rated Current	25A fuse model	DIN Min.	DIN Max.
600 %	0.099 s	0.02 s	0.1 s
350 %	0.34 s	0.04 s	0.5 s
200 %	3.9 s	0.15 s	5 s
135 %	110 s	0.75 s	1800 s

Table 4.2: Time to reach the melting point at given current

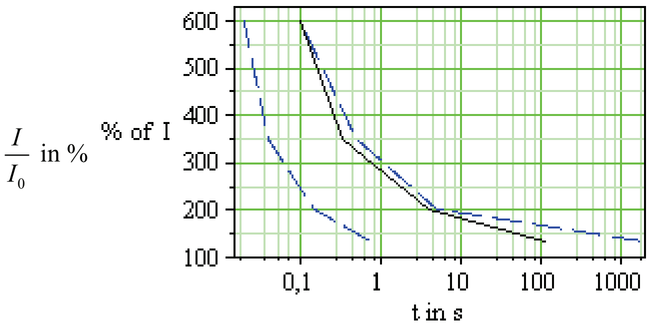

Fig. 4.10: Time-current curve of a 25A fuse

Temperature distribution in a fuse along *x*-axis is shown in Fig. 4.11. Fig. 4.12 shows steady-state temperature in the fuse at rated current of 25A.

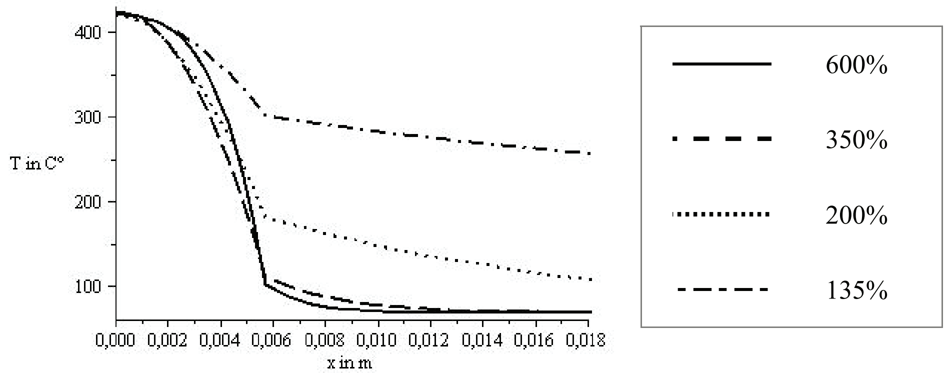

Fig. 4.11: Temperature distribution at different current values

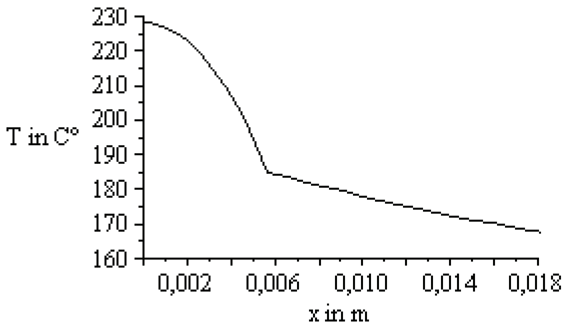

Fig. 4.12: Steady-state temperature at 25A current

It can be seen that the temperature is too high in the wire when the current is closer to nominal. Although we have isolation conditions on the right side of the model, that means that too much heat goes into the wires. Heat is generated not only by the fuse element but also by the fuse socket. Its heat generation power is higher than for wires.

Our proposal for future fuse design is to make a fuse socket with a larger cross-section and better heat convection properties on the surface. That will ensure that connected wires are not overheated and their insulation is not degraded.

4.5 Conclusions

In two steps, we approximated a cylindrical 3D mathematical model of the fuse and reduced it to a non-linear time-dependent system of three ordinary differential equations. This system is solvable with standard techniques. An approximate 3D solution could be analytically obtained from the solution of the transformed problem afterwards.

It is more efficient to calculate averaged mathematical problems rather than full 3D problems. A mathematical model could be used to calculate fuse breaking time and temperature distribution in the fuse. The geometry of a fuse-socket should be changed to improve fuse behaviour at nominal electric current.

5 Electro-welding

Industrial progress demands more and more raw material resources nowadays. Because they rise in price, new ways of saving resources are looked for, e.g., less expensive metal like aluminium is used in uncritical parts of long wires. Since aluminium is not suitable for mechanical contacts due to corrosion, materials like copper or brass have to be left in endings of the wires to use them in junctions and switches.

Electro-welding with a strong electric current is one of the original and most promising methods of joining two wires of different metals. Electric current is applied to wires that are put together until they melt and merge. It is important to reach melting temperature at the connection point in this process. To achieve this, the optimal length of both wire endings should be found.

5.1 Mathematical Model

The bare ends of wires are grabbed and held by clamps. A small part of the wire endings is left free, and they are put together to allow electric current to flow through and heat the material up. The temperature in holders is controlled by cooling them to a fixed temperature. The region of the wires between the clamps is considered.

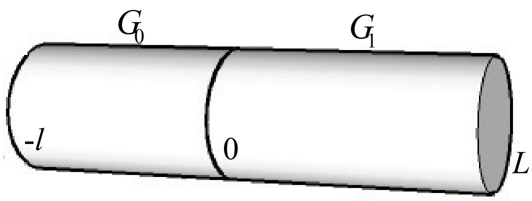

Fig. 5.1: Geometry of the model

Mathematical model consists of two joined cylinders G_0 and G_1 (Fig. 5.1) that represent connected wires:

$$G_0 = \{(x,r,\varphi) \mid x \in [-l,0], r \in [0,R], \varphi \in [0,2\pi]\},$$

$$G_1 = \{(x,r,\varphi) \mid x \in [0,L], r \in [0,R], \varphi \in [0,2\pi]\}.$$

We denote temperature in domain G_i as function $U_i(x,r,t)$, $t > 0$, $i = \overline{0,1}$. We assume rotational symmetry, i.e., temperature does not change over angle φ. Index i indicate corresponding sub-domain throughout this chapter.

Heat-up process is described by quasi-linear heat transfer equations:

$$\frac{\partial}{\partial t}(\gamma_i U_i) = \frac{\partial}{\partial x}\left(k_i \frac{\partial U_i}{\partial x}\right) + \frac{1}{r}\frac{\partial}{\partial r}\left(r k_i \frac{\partial U_i}{\partial r}\right) + F_i(U_i), \quad i = \overline{0,1}; \tag{1}$$

source functions F_i are linear and they describe heat generation by electric current:

$$F_i(U_i) = F_i(U_i(x,r,t)) = \frac{\rho_i\left(1+\alpha_{r,i}\left(U_i - U_r\right)\right)I^2}{A^2}. \tag{2}$$

Parameter ρ_i is resistivity of the material at the reference temperature U_r; $\alpha_{r,i}$ is temperature coefficient of electric resistivity; I – electric current; A – cross-section area of wire. Heat conductivity $k_i(U_i)$ and volumetric heat capacity $\gamma_i(U_i)$ are temperature dependent values.

We add conjugation conditions between cylinders, assuming continuity of temperature and heat flux:

$$U_0\big|_{x=0} = U_1\big|_{x=0}\,, \tag{3}$$

$$k_0\frac{\partial U_0}{\partial x}\bigg|_{x=-0} = k_1\frac{\partial U_1}{\partial x}\bigg|_{x=+0}\,. \tag{4}$$

Let us fix temperature at the endings

$$U_0\big|_{x=-l} = \theta\,, \tag{5}$$

$$U_1\big|_{x=L} = \theta\,; \tag{6}$$

and add boundary conditions on outer surface:

$$\left[k_i\frac{\partial U_i}{\partial r} + \alpha_i\left(U_i - \theta\right) + \varepsilon_i\sigma\left(U_i^4 - \theta^4\right)\right]\bigg|_{r=R} = 0\,, \quad i = \overline{0,1}\,; \tag{7}$$

where α_i is temperature-dependant non-linear heat convection coefficient, ε – emissivity of metal, σ – Stefan-Boltzmann constant, θ – ambient temperature.

We include also boundary conditions that define symmetry in the centre:

$$\frac{\partial U_i}{\partial r}\bigg|_{r=0} = 0\,, \quad i = \overline{0,1}\,; \tag{8}$$

and, after all, we add initial conditions:

$$U_i\big|_{t=0} = \theta\,, \quad i = \overline{0,1}\,. \tag{9}$$

5.2 Averaging over Radius *r*

Let us apply conservative averaging over radius r. We define integral averaged value in interval $[0, R]$:

$$w_i(x,t) = \frac{2}{R^2}\int_0^R rU_i(x,r,t)dr\,, \quad i = \overline{0,1}\,; \tag{10}$$

and assume constant temperature distribution in r-direction:

$$U_i(x,r,t) = w_i(x,t)\,. \tag{11}$$

Next, we integrate both sides of main differential equations (1):

$$\frac{2}{R^2}\int_0^R r\frac{\partial}{\partial t}\left(\gamma_i U_i\right)dr = \frac{2}{R^2}\int_0^R r\left[\frac{\partial}{\partial x}\left(k_i\frac{\partial U_i}{\partial x}\right) + \frac{1}{r}\frac{\partial}{\partial r}\left(rk_i\frac{\partial U_i}{\partial r}\right) + F_i(U_i)\right]dr \tag{12}$$

Let us look at the integration of the addends one by one.

1) $$\frac{2}{R^2}\int_0^R r\frac{\partial}{\partial t}\left(\gamma_i U_i\right)dr = \frac{\partial}{\partial t}\left(\frac{2}{R^2}\int_0^R r\gamma_i U_i dr\right) = \frac{\partial}{\partial t}\left(\gamma_i\frac{2}{R^2}\int_0^R rU_i dr\right) = \frac{\partial}{\partial t}\left(\gamma_i w_i\right).$$

First, the order of the integration and derivation could be switched because of the continuity of γ_i and U_i. Next, parameter γ_i could be brought outside integral because we assumed constant distribution of temperature over radius. Last, we obtain derivative of averaged function w_i using integral formula (10). Here, coefficient $\gamma_i = \gamma_i(w_i)$.

2) Similar transformations are done for the first addend of the right hand side:

$$\frac{2}{R^2}\int_0^R r\frac{\partial}{\partial x}\left(k_i\frac{\partial U_i}{\partial x}\right)dr \;=\; \frac{\partial}{\partial x}\left(k_i\frac{\partial}{\partial x}\left(\frac{2}{R^2}\int_0^R rU_i dr\right)\right) \;=\; \frac{\partial}{\partial x}\left(k_i\frac{\partial w_i}{\partial x}\right),$$

$$k_i = k_i(w_i).$$

3) Next term contains derivative in r-direction:

$$\frac{2}{R^2}\int_0^R \frac{\partial}{\partial r}\left(rk_i\frac{\partial U_i}{\partial r}\right)dr \;=\; \frac{2}{R^2}r\,k_i\frac{\partial U_i}{\partial r}\bigg|_0^R \;=\; \frac{2}{R}k_i\frac{\partial U_i}{\partial r}\bigg|_{r=R} \;=$$

$$=\frac{2}{R}\Big(-\alpha_i\left(U_i-\theta\right)-\varepsilon_i\sigma\left(U_i^4-\theta^4\right)\Big) \;=\; -\frac{2}{R}\Big(\alpha_i\left(w_i-\theta\right)+\varepsilon_i\sigma\left(w_i^4-\theta^4\right)\Big),$$

$$\alpha_i = \alpha_i(w_i).$$

Boundary condition (7) was used to substitute derivative, and function U_i could be substituted by w_i afterwards because of constant approximation (11).

4) Last term contains source function:

$$\frac{2}{R^2}\int_0^R rF_i(U_i)dr = F_i(w_i).$$

Consequently, differential equations (1) are the following after integration:

$$\frac{\partial}{\partial t}\left(\gamma_i w_i\right) = \frac{\partial}{\partial x}\left(k_i\frac{\partial w_i}{\partial x}\right) + \bar{F}_i(w_i), \quad i=\overline{0,1}; \tag{13}$$

where $\bar{F}_i(w_i) = -\frac{2}{R}\Big(\alpha_i\left(w_i-\theta\right)+\varepsilon_i\sigma\left(w_i^4-\theta^4\right)\Big)+F_i(w_i)$. (14)

Additional conditions are also integrated and result is similar to conditions of the original problem. We have conjugation conditions:

$$w_0\big|_{x=0} = w_1\big|_{x=0}, \tag{15}$$

$$k_0\frac{\partial w_0}{\partial x}\bigg|_{x=-0} = k_1\frac{\partial w_1}{\partial x}\bigg|_{x=+0}; \tag{16}$$

boundary conditions at the endings:

$$w_0\big|_{x=-l} = \theta, \tag{17}$$

$$w_1\big|_{x=L} = \theta; \tag{18}$$

and initial conditions:

$$w_i\big|_{t=0} = \theta, \quad i=\overline{0,1}. \tag{19}$$

Brand new statement of the 1D mathematical problem (Fig. 5.2) consists of differential equations (13) and additional conditions (15)-(19). Commonly, it is not possible to find analytical solution because of non-linearity. Numerical solution could be found using standard numerical techniques, e.g., methods of finite differences and factorization [37].

5.3 Averaging in *x*-direction Using Exponential Approximation

We have 1D mathematical problem now (Fig. 5.2). It is possible to reduce also the last space dimension by applying conservative averaging again.

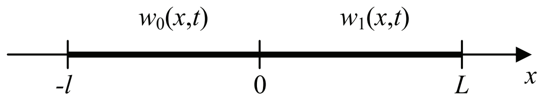

Fig. 5.2: Domain of a 1D mathematical problem

At first, we define integral averaged value function over each rod:

$$u_1(t) = \frac{1}{L}\int_0^L w_1(x,t)dx\,, \tag{20}$$

$$u_0(t) = \frac{1}{l}\int_{-l}^0 w_0(x,t)dx\,. \tag{21}$$

Let us assume exponential temperature distribution in *x*-direction as follows:

$$w_0(x,t) = u_0(t) + p_0(t)\left(\cosh\frac{x}{l} - \sinh 1\right) + q_0(t)\left(\sinh\frac{x}{l} + \cosh 1 - 1\right), \tag{22}$$

$$w_1(x,t) = u_1(t) + p_1(t)\left(\cosh\frac{x}{L} - \sinh 1\right) + q_1(t)\left(\sinh\frac{x}{L} - \cosh 1 + 1\right). \tag{23}$$

Expressions are written in such a way that they already fulfil integrals (20) and (21). p_0, p_1, q_0, q_1 are functions of time t that we will find from boundary and conjugation conditions. Parentheses around argument of hyperbolic functions are omitted from here onward, e.g.,

$$\sinh(x) = \sinh x\,; \quad \cosh(1) - 1 = \cosh 1 - 1\,; \quad \sinh(1)(a+b) = \sinh 1(a+b)\,.$$

Let us write down derivatives by argument x that we will use afterwards:

$$\frac{\partial w_0(x,t)}{\partial x} = \frac{1}{l}p_0(t)\sinh\frac{x}{l} + \frac{1}{l}q_0(t)\cosh\frac{x}{l}\,, \tag{24}$$

$$\frac{\partial w_1(x,t)}{\partial x} = \frac{1}{L}p_1(t)\sinh\frac{x}{L} + \frac{1}{L}q_1(t)\cosh\frac{x}{L}\,. \tag{25}$$

For simplicity, we omit also arguments of the functions in the next expressions.

From conjugation condition (15), we obtain:

$$u_0 + p_0(1-\sinh 1) + q_0(\cosh 1 - 1) = u_1 + p_1(1-\sinh 1) - q_1(\cosh 1 - 1)\,. \tag{26}$$

The second conjugation condition (16) gives the following:

$$\frac{\tilde{k}_0}{l}q_0 = \frac{\tilde{k}_1}{L}q_1\,; \tag{27}$$

where coefficients $\tilde{k}_i$ are at the point $x = 0$ here: $\tilde{k}_i = k_i(w_i(0,t))$.

From boundary conditions (17) and (18), we obtain:

$$u_0 + p_0\left(\cosh 1 - \sinh 1\right) + q_0\left(-\sinh 1 + \cosh 1 - 1\right) = \theta,$$

$$u_1 + p_1\left(\cosh 1 - \sinh 1\right) + q_1\left(\sinh 1 - \cosh 1 + 1\right) = \theta.$$

Let us convert constants with hyperbolic functions to exponential functions:

$$u_0 + \frac{1}{\mathrm{e}} p_0 - \left(1 - \frac{1}{\mathrm{e}}\right) q_0 = \theta, \tag{28}$$

$$u_1 + \frac{1}{\mathrm{e}} p_1 + \left(1 - \frac{1}{\mathrm{e}}\right) q_1 = \theta. \tag{29}$$

We obtain unknown functions by solving the system of four equations (26)-(29):

$$q_0(t) = D_0\left(u_1(t) - u_0(t)\right), \tag{30}$$

$$q_1(t) = D_1\left(u_1(t) - u_0(t)\right), \tag{31}$$

$$p_0(t) = D_0\left(\mathrm{e}-1\right)\left(u_1(t) - u_0(t)\right) - \mathrm{e}\left(u_0(t) - \theta\right), \tag{32}$$

$$p_1(t) = -D_1\left(\mathrm{e}-1\right)\left(u_1(t) - u_0(t)\right) - \mathrm{e}\left(u_1(t) - \theta\right); \tag{33}$$

where $D_0 = \dfrac{\mathrm{e}-1}{3-\mathrm{e}} \dfrac{\tilde{k}_1 l}{\tilde{k}_0 L + \tilde{k}_1 l}$,

$D_1 = \dfrac{\mathrm{e}-1}{3-\mathrm{e}} \dfrac{\tilde{k}_0 L}{\tilde{k}_0 L + \tilde{k}_1 l}$.

We can write down w_0 and w_1 now:

$$\begin{aligned} w_0(x,t) = u_0 + \left(D_0\left(\mathrm{e}-1\right)\left(u_1 - u_0\right) - \mathrm{e}\left(u_0 - \theta\right)\right)\left(\cosh\frac{x}{l} - \sinh 1\right) + \\ + D_0\left(u_1 - u_0\right)\left(\sinh\frac{x}{l} + \cosh 1 - 1\right), \end{aligned} \tag{34}$$

$$\begin{aligned} w_1(x,t) = u_1 - \left(D_1\left(\mathrm{e}-1\right)\left(u_1 - u_0\right) + \mathrm{e}\left(u_1 - \theta\right)\right)\left(\cosh\frac{x}{L} - \sinh 1\right) + \\ + D_1\left(u_1 - u_0\right)\left(\sinh\frac{x}{L} - \cosh 1 + 1\right). \end{aligned} \tag{35}$$

In fact, coefficients D_0 and D_1 also depend on time *t*, because they contain heat conduction coefficients k_0 and k_1.

Integration of differential equations (13) is the next step. The first integral is in interval $(-l, 0)$; the second one – in interval $(0, L)$:

$$\frac{1}{l}\int_{-l}^{0} \frac{\partial}{\partial t}\left(\gamma_0 w_0\right) dx = \frac{1}{l}\int_{-l}^{0} \left[\frac{\partial}{\partial x}\left(k_0 \frac{\partial w_0}{\partial x}\right) + \bar{F}_0(w_0)\right] dx, \tag{36}$$

$$\frac{1}{L}\int_{0}^{L} \frac{\partial}{\partial t}\left(\gamma_1 w_1\right) dx = \frac{1}{L}\int_{0}^{L} \left[\frac{\partial}{\partial x}\left(k_1 \frac{\partial w_1}{\partial x}\right) + \bar{F}_1(w_1)\right] dx. \tag{37}$$

Let us look at the integration of the addends one by one again.

1) On the left hand side, we change order of derivation and integration and use mean value theorem as described at the end of Section 3.4:

$$\frac{1}{l}\int_{-l}^{0}\frac{\partial}{\partial t}(\gamma_0 w_0)\,dx=\frac{d}{dt}\left[\frac{1}{l}\int_{-l}^{0}\gamma_0 w_0 dx\right]\cong\frac{d}{dt}\left[\tilde{\gamma}_0\frac{1}{l}\int_{-l}^{0}w_0 dx\right]=\frac{d}{dt}(\tilde{\gamma}_0 u_0);$$

where averaged value is used to calculate heat capacity: $\tilde{\gamma}_0(t)=\gamma_0(u_0)$.

2) We use our approximating functions (34) and (35) to change derivatives of x in the first term of the right hand side:

$$\frac{1}{l}\int_{-l}^{0}\left[\frac{\partial}{\partial x}\left(k_0\frac{\partial w_0}{\partial x}\right)\right]dx=\frac{1}{l}\left(k_0\frac{\partial w_0}{\partial x}\right)\Bigg|_{-l}^{0}=\frac{1}{l}\left(\tilde{k}_0\frac{\partial w_0}{\partial x}\bigg|_{x=0}-\overline{k}_0\frac{\partial w_0}{\partial x}\bigg|_{x=-l}\right)=$$

$$=\frac{1}{l^2}\left[\tilde{k}_0 q_0-\overline{k}_0(-p_0\sinh 1+q_0\cosh 1)\right]=\frac{1}{l^2}\left[\tilde{k}_0 D_0(u_1-u_0)-\right.$$

$$\left.-\overline{k}_0\left(-\sinh 1\left(D_0(\mathrm{e}-1)(u_1-u_0)-\mathrm{e}(u_0-\theta)\right)+D_0\cosh 1(u_1-u_0)\right)\right]=$$

$$=\frac{1}{l^2}\left[D_0\left(\tilde{k}_0-\overline{k}_0\left(\cosh 1-\sinh 1(\mathrm{e}-1)\right)\right)(u_1-u_0)-\mathrm{e}\,\overline{k}_0\sinh 1(u_0-\theta)\right];$$

where $\tilde{k}_0(t)=k_0(w_0(0,t))$ and $\overline{k}_0(t)=k_0(w_0(-l,t))$.

3) Last term to integrate is source function $\overline{F}_0$. In general, it is non-linear and it is impossible to find integral analytically. Suggestion is to use averaged value for calculations. Additional research should be done to find more precise procedure for calculation of coefficients; and how does it influences solution:

$$f_0(t):=\frac{1}{l}\int_{-l}^{0}\overline{F}_0(w_0)dx\cong\overline{F}_0(u_0).$$

Similar conversions could be done to the second differential equation (37); and we can write down our new 0D mathematical problem. It consists of two ordinary differential equations (38)-(39) that depend only on time t:

$$\frac{d}{dt}(\tilde{\gamma}_0 u_0)=E_1(u_1-u_0)+E_2(u_0-\theta)+f_0,\tag{38}$$

$$\frac{d}{dt}(\tilde{\gamma}_1 u_1)=E_3(u_1-u_0)+E_4(u_1-\theta)+f_1;\tag{39}$$

and initial conditions:

$$u_i\big|_{t=0}=\theta,\quad i=\overline{0,1}.\tag{40}$$

Here, $E_1=\frac{1}{l^2}D_0\left(\tilde{k}_0-\overline{k}_0\left(\cosh 1-\sinh 1(\mathrm{e}-1)\right)\right)$, $\quad E_2=-\frac{1}{l^2}\mathrm{e}\,\overline{k}_0\sinh 1$,

$E_3=-\frac{1}{L^2}D_1\left(\tilde{k}_1-\overline{k}_1\left(\cosh 1-\sinh 1(\mathrm{e}-1)\right)\right)$, $\quad E_4=-\frac{1}{L^2}\mathrm{e}\,\overline{k}_1\sinh 1$,

$\tilde{k}_i(t)=k_i(w_i(0,t))$, $\quad \overline{k}_0(t)=k_0(w_0(-l,t))$, $\quad \overline{k}_1(t)=k_1(w_1(L,t))$.

When solution of these equations is found, approximated solution of the original problem can be obtained by formulae (11), (22), (23).

5.4 Alternative Averaging in *x*-direction Using Polynomial Approximation

Let us use another approximation functions over x instead of functions (22) and (23):

$$w_0(x,t) = u_0(t) + \hat{q}_0(t)\left(\frac{x}{l} + \frac{1}{2}\right) + \hat{p}_0(t)\left(\left(\frac{x}{l}\right)^2 - \frac{1}{3}\right), \tag{41}$$

$$w_1(x,t) = u_1(t) + \hat{q}_1(t)\left(\frac{x}{L} - \frac{1}{2}\right) + \hat{p}_1(t)\left(\left(\frac{x}{L}\right)^2 - \frac{1}{3}\right). \tag{42}$$

These equations already fulfil integrals (20) and (21). We can obtain unknown functions using boundary conditions (15)-(18):

$$\hat{q}_0(t) = \frac{6(u_1 - u_0)}{1+m}, \quad \hat{p}_0(t) = \frac{3}{2}\left(\frac{3(u_1 - u_0)}{1+m} - (u_0 - \theta)\right),$$

$$\hat{q}_1(t) = \frac{6m(u_1 - u_0)}{1+m}, \quad \hat{p}_1(t) = \frac{3}{2}\left(\frac{3m(u_0 - u_1)}{1+m} - (u_1 - \theta)\right), \quad m = \frac{L\tilde{k}_0}{l\tilde{k}_1}.$$

Integration of differential equations (13) over corresponding intervals gives system of ordinary differential equations:

$$\frac{d}{dt}(\tilde{\gamma}_0 u_0) = \frac{3}{l^2}\left(\frac{2\tilde{k}_0 - \overline{k}_0}{1+m}(u_1 - u_0) - \overline{k}_0(u_0 - \theta)\right) + f_0, \tag{43}$$

$$\frac{d}{dt}(\tilde{\gamma}_1 u_1) = \frac{3}{L^2}\left(m\frac{2\tilde{k}_1 - \overline{k}_1}{1+m}(u_0 - u_1) - \overline{k}_1(u_1 - \theta)\right) + f_1. \tag{44}$$

Adding initial conditions (40) to the last two equations gives another system of ordinary differential equations besides (38)-(40). These systems of equations are simplified mathematical models of our original problem.

5.5 Numerical Results

Research in the field of electro-welding began only recently and there is no experimental praxis how this could be done in the most efficient way (in terms of dimensions, applied current etc.). One of the demands in industry is joining brass and aluminium wires. The latter material is cheaper and it is used in longer parts of wires, while the first has better properties and is used in more complex parts of electric systems.

Let us take aluminium wire of radius $R_{Al} = 0.895mm$ and join it with brass wire of radius $R = 1.175mm$. The end of the aluminium wire is covered by a brass sleeve in such a way that the radius is the same as for the brass wire. In our model (Fig. 5.1), we assume that aluminium is on the left hand side, but brass – on the right hand side.

Because aluminium wire has a brass sleeve, mixed properties should be taken for that part of the model. Coefficients are calculated in proportion to cross-section areas (for electric resistivity – in inverse proportion):

$$k_0(U_0) = pk_{Al}(U_0) + (1-p)k_1(U_0),$$
$$\gamma_0(U_0) = p\gamma_{Al}(U_0) + (1-p)\gamma_1(U_0),$$
$$F_0(U_0) = \frac{I^2}{A^2}\left(\frac{p}{\rho_{Al}\left(1+\alpha_{r,Al}\left(U_0-U_r\right)\right)} + \frac{(1-p)}{\rho_1\left(1+\alpha_{r,1}\left(U_0-U_r\right)\right)}\right);$$

where $p = R_{Al}^2 / R^2$, $A = \pi R^2$.

Physical properties of aluminium and brass are as follows [26]:

a) heat conductivity k_{Al} and k_1: Fig. 5.3;

b) volumetric heat capacity γ_{Al} and γ_1: Fig. 5.4 (constant value is used for brass);

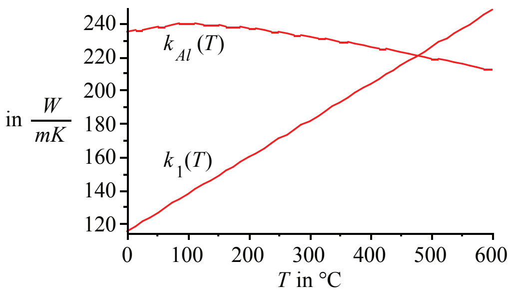

Fig. 5.3: Heat conductivity of aluminium and brass

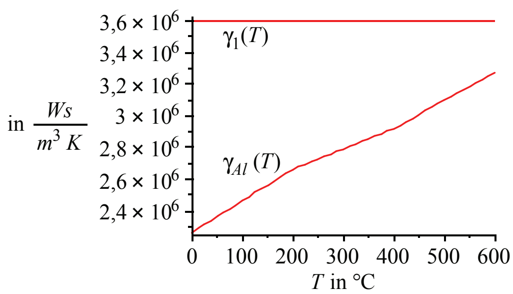

Fig. 5.4: Volumetric heat capacity of aluminium and brass

c) resistivity at the reference temperature $U_r = 20°C$:

$\rho_{Al} = 2.668 \cdot 10^8 \Omega m$, $\rho_1 = 6.667 \cdot 10^8 \Omega m$;

d) temperature coefficient of electric resistivity:

$\alpha_{r,Al} = 4.31 \cdot 10^{-3} \cdot 1/K$, $\alpha_{r,1} = 1.7 \cdot 10^{-3} \cdot 1/K$;

e) free convection coefficient $\alpha(T) := \alpha_0(T) = \alpha_1(T)$ for round wire of radius R in air ($\theta = 20°C$):

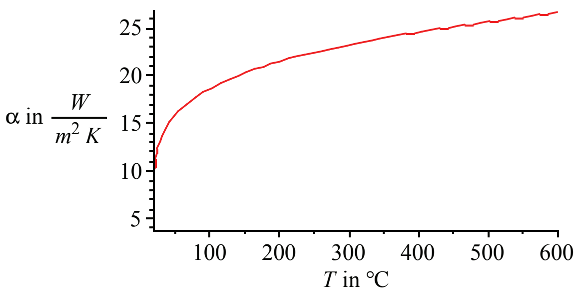

Fig. 5.5: Free convection coefficient for the surface of a round wire

f) surface emissivity (because of the sleeve, we need it only for brass):

$\varepsilon := \varepsilon_0 = \varepsilon_1 = 0.035$, $\sigma = 5.6704 \cdot 10^{-8}\, W/m^2K^4$;

g) temperature to reach (aluminium melting temperature because it is lower than for brass): $T_{Al} = 660°C$;

Let us apply 900A strong electric current to our connected wires. If the length of each part is equal to 10mm, melting temperature is reached inside the brass wire and not at the connection point (Fig. 5.6 – 1D PDE model used. Vertical line shows where maximum temperature is). To shift the maximum point, the dimensions should be changed, e.g., aluminium part could be made longer.

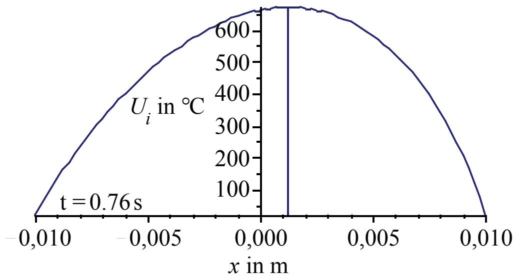

Fig. 5.6: Temperature profile if length of wire endings is equal

At first, let us neglect heat convection and radiation and use other parameters as constants. Table 5.1 shows how long should be the length of aluminium part of the model to reach melting temperature at the connection point. Results are obtained by 1D PDE model and two ODE models from previous sections of this chapter. Parameters are calculated at average temperature of 327°C (600 K).

Model	Length *l*	Time *t*
1D PDE system	14.4 mm	0.67 s
ODE system with exponential approx.	14.3 mm	0.56 s
ODE system with polynomial approx.	14.7 mm	0.52 s

Table 5.1: Length of the endings to start melting at the connection. Constant parameters

Calculated lengths are almost the same among models, while time value of ODE systems differs by 16-22% from 1D model.

Fig. 5.7 shows temperature distribution along *x*-axes at the time moments when melting point is reached for each considered mathematical model.

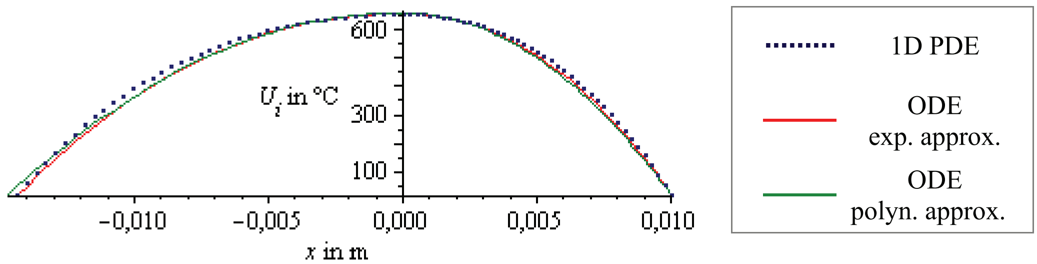

Fig. 5.7: Temperature profile by different mathematical models. Constant parameters

Next, we use temperature-dependent coefficients and take into account heat convection and radiation. PDE model gives length of 15.8 *mm* of aluminium wire that is by 10% more than before. Time to reach melting temperature stays the same: $t = 0.67\ s$.

Finding optimal length by ODE systems fails. Maximum point tends to junction of the wires but do not reach it however large the length l is. Such effect is caused mostly by calculation of transient heat conductivity coefficient k. If it is computed from averaged values, i.e. $\tilde{k}_i = \overline{k}_i = k_i(u_i(t))$ in formulae (38)-(39) and (43)-(44), solution for optimal length can be found (Table 5.2). If we compare results with 1D solution, length is longer by 5% in case of exponential approximation and by 20% in case of polynomial approximation.

Model	Length *l*	Time *t*
1D PDE system	15.8 mm	0.67 s
ODE system with exponential approx.	16.6 mm	0.63 s
ODE system with polynomial approx.	19.0 mm	0.59 s

Table 5.2: Length of the endings to start melting at the connection. Transient parameters

Fig. 5.8 shows temperature distribution in wires obtained by all three models at the moment of reaching melting temperature.

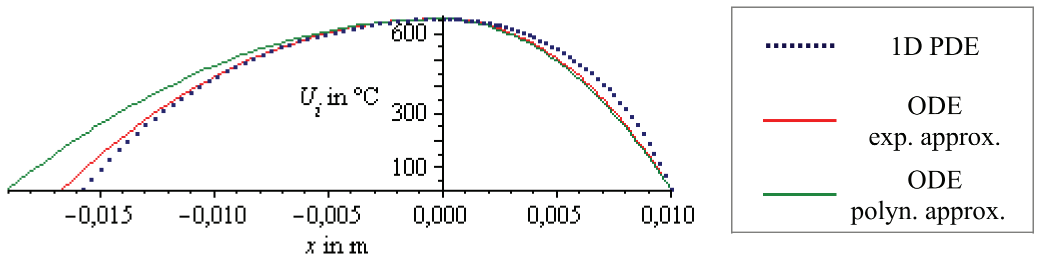

Fig. 5.8: Temperature profile by different mathematical models. Transient parameters

5.6 Conclusions

For the presented physical situation, a mathematical model was constructed that consisted of two 3D cylinders and a description of electro-thermal properties. Using the conservative averaging approach, it was approximated and reduced to a one-dimensional model and also to two kinds of zero-dimensional mathematical models.

Since experimental data from manufacturer was not available at the time of writing this thesis, approbation and improvement of the current mathematical model will take place at a later collaboration stage. For example, a more complex geometry of the model could be considered because initially it was not known that the ending of the aluminium wire has a brass sleeve.

Additional research should be done to determine the observed behaviour of numerical solutions of ODE systems, i.e., whether the significant influence of parameter approximation is due to averaging over an interval where the coefficient is not monotone (Fig. 5.3), or due to the usage of a difference scheme, or another reason.

This chapter could be used as an example for applying the conservative averaging method to other cylindrical mathematical models, e.g., cooling systems with cylindrical fins.

Conclusion

Efficient mathematical models of several industrial problems were developed during this research, fulfilling the goal of the Ph.D. thesis. International collaboration with Munich Bundeswehr University gave an opportunity to work on the topical issues of today. The conservative averaging method allowed the creation of fast mathematical models and the accomplishment of many calculations in a short period of time. Quick computation helped to better form a sort of sense about processes in the considered problems, and to create ideas for their further development.

Specialists from different fields contributed to the problems researched – mathematicians, engineers, physicists. Multidisciplinary cooperation is needed nowadays because the investigated problems often are too complicated to be solved with the knowledge of a single person's specialisation. Another important connection is the link between scientists and industry, turning research results into innovations. This should be the main reason that drives the progress and development of countries including Latvia. Above all, let us hope that, through helping to obtain a deeper understanding of natural laws, science in general will remain friendly to the earth and humanity.

Bibliography

[1] *Aufgabenstellung und Lősung einer Klasse von Problemen der mathematischen Physik mit nichtklassischen Zusatzbedingungen.* **Buikis A.** 1984, Rostocker Mathematisches Kolloquium, Bd. 25, S. 53-62. In German.

[2] *The Change of Formulation of Problems of Mathematical Physics with Discontinuous Coefficients in Compound Domains.* **Buikis A.** 1986, The Electronic Modelling, Vol. 8, Issue 6, pp. 81-83. In Russian.

[3] **Buikis A.** *Modelling of Filtration Processes in Layered Porous Media by the Conservative Averaging Method.* Kazan, 1987. 374 p., Dr. Thesis. In Russian.

[4] *Simulation of steady-state heat process for the rectangular fin-containing system.* **Buiķe M.** Vilnius : Technika, 1999, Mathematical Modelling and Analysis, Vol. 4, pp. 33-43. ISSN 1648-3510.

[5] *Some Approximate Analytical Steady-State Solutions for Cylindrical Fin.* **Bruvere A. and Buikis A.** Athens : WSEAS Press, 2006. Proceedings of the 4th IASME/WSEAS Int. Conf on Heat Transfer, Thermal Engineering and Environment. Elounda, Crete Island, Greece, August 21-23, 2006. pp. 238-243.

[6] *Analytical 3-D Steady-State Statement for Cylindrical Fin and some of it's Approximate Solutions.* **Buikis A. and Bruvere A.** Athens : WSEAS Press, 2006, WSEAS Transactions on Heat and Mass Transfer, Vol. 1, Issue 4. ISSN 1790-5044.

[7] *The mathematical model of the plywood production.* **Buikis A., Cepitis J. and Kostjukova S.** Athens : WSEAS Press, 2008. Proc. of the 13th WSEAS Int. Conf. on Applied Mathematics (MATH'08). ISSN: 1790-2769.

[8] *Modelling of the Convective Diffusion Process with Nonlinear Sorption in Multi-Layered Aquifer.* **Buikis A., Rusakevich Z. and Ulanova N.** Dordrecht, Boston, London : Kluwer Academic Publishers, 1995, Transport in Porous Media, Vol. 19, Issue 1, pp. 1-13. ISSN 0169-3913.

[9] *Approximate Solutions of Heat Conduction Problems in Multi-dimensional Cylinder Type Domain by Conservative Averaging Method, Part 1.* **Buike M. and Buikis A.** Athens : WSEAS Press, 2007. Proc. of the 5th IASME/WSEAS Int. Conf. on Heat Transfer, Thermal Engineering and Environment (HTE'07). pp. 15-20.

[10] *Several Intensive Steel Quenching Models for Rectangular Samples.* **Buike M. and Buikis A.** Athens : WSEAS Press, 2010. Latest Trends on Theoretical and Applied Mechanics, Fluid Mechanics and Heat & Mass Transfer. Int. Conf. on Fluid Mechanics and Heat & Mass Transfer. Corfu Island, Greece, July 22-24, 2010. pp. 88-93. ISBN 978-960-474-211-0.

[11] *Definition and Calculation of a Generalized Integral Parabolic Spline.* **Buikis A.** 1995, Proceedings of the Latvian Academy of Sciences. Section B, No. 7/8, pp. 97-100.

[12] **Buikis A. and Ulanova N.** Analytically-numerical method for temperature fields in multilayered system. [ed.] B. Sunden and C.A. Brebbia. *Advanced Computational Methods in Heat Transfer VI.* Southampton, Boston : WIT Press, 2000, pp. 445-453.

[13] *Mathematical Model for Diffusion-Sorption Processes in Layered Strata with Interlayers.* **Kostjukova S. and Buikis A.** Athens : WSEAS Press, 2007. 5th WSEAS Int. Conf. on Environment, Ecosystems and Development. Tenerife, Spain, December 14-16, 2007. pp. 7-12.

[14] *Integral Rational Spline with Jump for Discontinuous Mathematical Problems in Layered Media.* **Kostjukova S. and Buikis A.** Athens : WSEAS Press, 2010. Latest Trends on Theoretical and Applied Mechanics, Fluid Mechanics and Heat & Mass Transfer. Int. Conf. on Fluid Mechanics and Heat & Mass Transfer. Corfu Island, Greece, July 22-24, 2010. pp. 137-141. ISSN: 1792-4359.

[15] **Vilums R.** *Estimates of Approximation Errors for Conservative Averaging Method.* Faculty of Physics and Mathematics. Rīga : University of Latvia, 2004. 90 p., Master Thesis. In Latvian.

[16] **Ilgevicius A.** *Analytical and Numerical Analysis and Simulation of Heat Transfer in Electrical Conductors and Fuses.* Neubiberg : Universität der Bundeswehr München, 2004. Dissertation.

[17] *Calculation of the Heat Transfer in Cylindrical Wires and Electrical Fuses by Implicit Finite Volume Method.* **Ilgevicius A. and Liess H.-D.** 2003, Mathematical Modelling and Analysis, Vol. 8, Issue 3, pp. 217-228.

[18] *Fuses for Automotive Application.* Des Plaines, Il60016, U.S.A. : Littelfuse Inc.

[19] *Thermal Processes in SF6-filled Fuses Below the Minimum Melting Current.* **Brechtken D., Konig D. and Muller B.** Nottingham : s.n., 1991. Proceedings of the 4th International Conference on Electric Fuses and their Applications.

[20] *Transient Heat Conduction in 3D Fuse Modeled by Conservative Averaging Method.* **Vilums R. and Buikis A.** Athens : WSEAS Press, 2007. Proceedings of the 3rd WSEAS Int. Conf. on Applied and Theoretical Mechanics (Mechanics ’07). Puerto De La Cruz, Spain, December 14 – 16, 2007. pp. 54-59.

[21] Post-Conference Report for the WSEAS Conferences: E-ACTIVITIES '07, ISP '07, CIMMACS '07, ELECTROSCIENCE '07, EED'07, and MECHANICS'07. *WSEAS.* [Online] [Cited: May 8, 2010.] http://www.wseas.us/reports/2007/tenerife/.

[22] *Modelling of Three-Dimensional Transport Processes in Anisotropic Layered Stratum by Conservative Averaging Method.* **Buike M. and Buikis A.** Athens : WSEAS Press, 2006, WSEAS Transactions on Heat and Mass Transfer, Vol. 1, Issue 4, pp. 430-437.

[23] *System of Various Mathematical Models for Transport Processes in Layered Strata with Interlayers.* **Buike M. and Buikis A.** Athens : WSEAS Press, 2007, WSEAS Transactions on Mathematics, Vol. 6, Issue 4, pp. 551-558.

[24] **Buikis A.** Conservative Averaging as an Approximate Method for Solution of Some Direct and Inverse Heat Transfer Problems. *Advanced Computational Methods in Heat Transfer, IX.* Southampton : WIT Press, 2006, pp. 311-320.

[25] **Buikis A.** *Problems of Mathematical Physics with Discontinuous Coefficients and Their Applications.* Rīga : s.n., 1991. 385 p. In Russian, unpublished book.

[26] *VDI-Wärmeatlas.* 9. Aufl. Berlin : Springer, 2002.

[27] **Dvorsky K., Gwinner J. and Liess H.-D.** *Heat Conduction in Insulated Circular Mains.* Department of Aerospace Engineering; Department of Electrical Engineering and Information Technology. Neubiberg/Munich : Universität der Bundeswehr München, 2009. Preprint.

[28] *Numerical Simulation of the Heat Conduction in Electrical Cables.* **Ciegis R., Ilgevicius A., Liess H.-D., et al.** Vilnius : Technika, 2007, Mathematical Modelling and Analysis, Vol. 12, Issue 4, pp. 425-439. ISSN 1648-3510.

[29] *Numerical Method for the Inverse Heat Transfer Problem in Composite Materials with Stefan-Boltzmann Conditions.* **Hu X., Xu X. and Chen W.** New York : Springer U.S., 2010, Advances in Computational Mathematics, Vol. 33, Issue 4, pp. 471-489. ISSN 1019-7168, DOI 10.1007/s10444-009-9131-x.

[30] *Numerical Simulation of the Heat Conduction in Composite Materials.* **Ciegis R., Jankeviciute G. and Suboc O.** Vilnius : Technika, 2010, Mathematical Modelling and Analysis, Vol. 15, Issue 1, pp. 9-22.

[31] *Numerical Simulation of Heat Distribution in a Current-Carrying Multi Wire.* **Loos F. and Liess H.-D.** 2010. Abstracts of MMA2010, May 26 - 29, 2010, Druskininkai, Lithuania. p. 63. http://inga.vgtu.lt/~art/konf/MMA15_Abstracts.pdf.

[32] **Kern D.Q. and Kraus A.D.** *Extended Surface Heat Transfer.* New York : McGraw-Hill, 1972. 816 p.

[33] **Manzoor M.** *Heat Flow through Extended Surface Heat Exchangers.* Berlin and New York : Springer-Verlag, 1984. 286 p.

[34] *Performance Indicators for Steady-State Heat Transfer Through Fin Assemblies.* **Wood A.S., Tupholme G.E., Bhatti M.I.H., et al.** New York : ASME, 1996, Journal of Heat Transfer, Vol. 118, Issue 2, pp. 310-316.

[35] **Ockendon J., Howison S., Lacey A., et al.** *Applied Partial Differential Equations.* New York : Oxford University Press, USA, 1999. 440 p.

[36] **Incropera F.P.** *Fundamentals of Heat and Mass Transfer.* 6th ed. Hoboken (NJ) : Wiley, 2006. 1024 p.

[37] **Samarskii, A. A.** *The Theory of Difference Schemes.* Boca Raton (FL) : CRC Press, 2001. 786 p.

[38] **Samarskii, A. A. and Vabishchevich, P. N.** *Computational Heat Transfer, Volume 1, Mathematical Modelling.* Hoboken (NJ) : Wiley, 1995. 418 p.

Appendix 1 Finite Difference Method for 1D Problem

Systems of quasi-linear partial differential equations in a one space dimension were considered in chapters 3 to 5. A finite difference method was used to calculate them numerically. The mathematical models consisted of several sub-domains that were connected by conjugation conditions. This chapter shows how to obtain finite differences with a second order of approximation in space, including a conjugation point.

App 1.1 Statement of the 1D Problem

The system of quasi-linear 1D heat equations has the form as follows:

$$\frac{\partial}{\partial t}\left(\gamma_j(w_j)w_j\right)=\frac{\partial}{\partial x}\left(k_j(w_j)\frac{\partial w_j}{\partial x}\right)+f_j(x,t,w_j),\quad w_j=w_j(x,t),\, x\in[x_j,x_{j+1}]\,;\,(1)$$

where j is the index of the equation. Source functions $f_j(x,t,w_j)$ play the role of the heat sources or heat sinks.

As an example, let us take mathematical model of the automotive fuse (39)-(42) from Chapter 3.6. Then:

$$x_0=0,\quad x_1=l,\quad x_2=l+L,\quad k_0=k_1=k,\quad \gamma_0=\gamma_1=\gamma\,,\quad j=\overline{0,1}\,;$$

and source functions are the following:

$$\begin{aligned} f_0(x,t,w_0)&=B_0\left(1+\alpha_r\left(w_0-U_r\right)\right)-h_0\left(\frac{1}{b}+\frac{1}{h}\right)\left(w_0-\Theta\right),\\ f_1(x,t,w_1)&=B_1\left(1+\alpha_r\left(w_1-U_r\right)\right)-h_1\left(\frac{1}{b}+\frac{1}{H}\right)\left(w_1-\Theta\right).\end{aligned}\qquad(2)$$

Boundary conditions are taken as the generalization of the homogeneous boundary conditions (40):

$$k\left.\frac{\partial w_0}{\partial x}\right|_{x=0}=q_0(t),\quad k\left.\frac{\partial w_1}{\partial x}\right|_{x=l+L}=q_1(t).\qquad(3)$$

Conjugation conditions differ from the ideal thermal contact conditions as well as from non-ideal thermal contact conditions:

$$\left.w_0\right|_{x=l-0}=\left.w_1\right|_{x=l+0},\qquad(4)$$

$$hk\left.\frac{\partial w_0}{\partial x}\right|_{x=l-0}=\left.\left[Hk\frac{\partial w_1}{\partial x}-h_1\left(H-h\right)\left(w_1-\Theta\right)\right]\right|_{x=l+0}.\qquad(5)$$

Initial conditions can be non-homogeneous:

$$\left.w_0\right|_{t=0}=\left.w_1\right|_{t=0}=U^0(x).\qquad(6)$$

From mathematical point of view, important is a fact that the functions $f_j(x,t,w_j)$ (as well as functions $\gamma(w_j)$) fulfil following estimations:

$$\left|\frac{\partial f_j(x,t,w_j)}{\partial w_j}\right| \le M, \quad \left|\frac{\partial \gamma}{\partial w_j}\right| \le M, \quad j=\overline{0,1}, \quad M \in R.$$

These constraints guarantee the uniqueness of the solution of the problem (1)-(6).

App 1.2 Construction of the Finite Difference Scheme

Finite difference method for heat transfer problems are well explained in literature, e.g. [38]. The finite difference solution of the 1D problem will be denoted as $v_{j,i}^n \approx w_j(x_i,t_n)$. We will use uniform time step: $t_n = n\tau$, $n=\overline{0,N}$; the space step will be piece-wise constant:

$$x_i = i\Delta x_0, \quad i=\overline{0,i_0}, \quad \Delta x_0 = \frac{l}{i_0};$$

$$x_i = l + (i-i_0)\Delta x_1, \quad i=\overline{i_0,i_1}, \quad \Delta x_1 = \frac{L-l}{i_1-i_0}.$$

We approximate heat conductivity term of the equation (1) by difference operator as follows (temporarily, we omit the notation of the time-level n and function index j):

$$\Lambda v_i = [k(v)_i[v_i]_{\bar{x}}]_x, \quad i \ne 0, i_0, i_1. \tag{7}$$

Here, we have used traditional notation, e.g. [38]:

$$[v_i]_{\bar{x}} = \frac{v_i - v_{i-1}}{\Delta x}, \quad [v_i]_x = \frac{v_{i+1}-v_i}{\Delta x};$$

where $\Delta x = \Delta x_0,\ 0<i<i_0;\ \Delta x = \Delta x_1,\ i_0<i<i_1.$

Difference operator (7) could be rewritten in the following form:

$$[k(v)_i[v_i]_{\bar{x}}]_x = \frac{k(v)_{i+1}v_{i+1} - (k(v)_i + k(v)_{i+1})v_i + k(v)_i v_{i-1}}{\Delta x^2}. \tag{8}$$

For coefficient $k(v)_i$, several equivalent expressions can be applied in the sense of the order of approximation $O(\Delta x^2)$, e.g.

$$k(v)_i = k\left(\frac{v_i + v_{i-1}}{2}\right) \tag{9}$$

or $$k(v)_i = \frac{k(v_{i-1}) + k(v_i)}{2}. \tag{10}$$

Now, we can propose two-step *predictor-corrector-type* finite difference scheme for the differential equations (1) (it is important to show the time-level here again):

$$\gamma(v_i^n)\frac{\tilde{v}_i^{n+1} - v_i^n}{\tau} = [k(v^n)_i[\tilde{v}_i^{n+1}]_{\bar{x}}]_x + f(x,t,v)_i^n,$$

$$\gamma(\tilde{v}_i^n)\frac{v_i^{n+1} - v_i^n}{\tau} = [k(\tilde{v}^{n+1})_i[v_i^{n+1}]_{\bar{x}}]_x + f(x,t,\tilde{v})_i^{n+1}; \tag{11}$$

$$0<i<i_0,\ i_0<i<i_1 \ \left(i\ne 0,\ i\ne i_0,\ i\ne i_1\right).$$

Next, we will pay special attention to obtain approximation of the boundary conditions (3) and conjugations conditions (4), (5) with the same order of approximation $O(\Delta x^2)$ as the finite difference equations (11). To guaranty the second order of the approximation, we employ the idea of using the main differential equation on the border [37]. We start with Taylor series expansions for the functions $v^n_{j,i}$ as differentiable functions of arguments x and t:

$$k_i v_{i\pm 1} = k_i v_i \pm \Delta x\, k_i \left.\frac{\partial v}{\partial x}\right|_i + \frac{\Delta x^2}{2} k_i \left.\frac{\partial^2 v}{\partial x^2}\right|_i + O(\Delta x^3); \qquad \left.\frac{\partial v}{\partial x}\right|_i := \left.\frac{\partial v}{\partial x}\right|_{x=x_i}.$$

Important nuance is that the heat conductivity coefficient k is taken at the fixed point $x = x_i$: $k_i = k(x_i)$. This assumption allows us to rewrite the last formula as follows:

$$k_i v_{i\pm 1} = k_i v_i \pm \Delta x\, k_i \left.\frac{\partial v}{\partial x}\right|_i + \frac{\Delta x^2}{2} \frac{\partial}{\partial x}\left.\left(k \frac{\partial v}{\partial x}\right)\right|_i + O(\Delta x^3). \tag{12}$$

Next two equalities follow from (12):

$$k_i \left.\frac{\partial v}{\partial x}\right|_i = k_i \frac{v_i - v_{i-1}}{\Delta x} + \frac{\Delta x}{2} \frac{\partial}{\partial x}\left.\left(k \frac{\partial v}{\partial x}\right)\right|_i + O(\Delta x^2),$$

$$k_i \left.\frac{\partial v}{\partial x}\right|_i = k_i \frac{v_{i+1} - v_i}{\Delta x} - \frac{\Delta x}{2} \frac{\partial}{\partial x}\left.\left(k \frac{\partial v}{\partial x}\right)\right|_i + O(\Delta x^2).$$

The assumption that functions $v(x,t)$ fulfil differential equations (1) gives next expressions for the first-order derivatives:

$$k_i \left.\frac{\partial v}{\partial x}\right|_i = k_i \frac{v_i - v_{i-1}}{\Delta x} + \frac{\Delta x}{2} \left.\left[\frac{\partial}{\partial t}(\gamma v) - f(x,t,v)\right]\right|_i + O(\Delta x^2), \tag{13}$$

$$k_i \left.\frac{\partial v}{\partial x}\right|_i = k_i \frac{v_{i+1} - v_i}{\Delta x} - \frac{\Delta x}{2} \left.\left[\frac{\partial}{\partial t}(\gamma v) - f(x,t,v)\right]\right|_i + O(\Delta x^2). \tag{14}$$

It remains to apply these equations to the boundary conditions (3), and, in accordance with difference scheme (11), we obtain second order finite difference approximation of both boundary conditions. We have the following difference equations for the predictor step:

$$\begin{aligned} &\frac{\Delta x_0}{2}\gamma(v^n_{0,0})\frac{\tilde v^{n+1}_{0,0} - v^n_{0,0}}{\tau} - k(v^n_{0,0})[\tilde v^{n+1}_{0,0}]_x = \frac{\Delta x_0}{2} f_0(x_0, t_n, v^n_{0,0}) - q_0(t_n), \\ &\frac{\Delta x_1}{2}\gamma(v^n_{1,i_1})\frac{\tilde v^{n+1}_{1,i_1} - v^n_{1,i_1}}{\tau} + k(v^n_{1,i_1})[\tilde v^{n+1}_{1,i_1}]_{\bar x} = \frac{\Delta x_1}{2} f_1(x_{i_1}, t_n, v^n_{1,i_1}) + q_1(t_n); \end{aligned} \tag{15}$$

and difference equations for the corrector step:

$$\begin{aligned} &\frac{\Delta x_0}{2}\gamma(\tilde v^{n+1}_{0,0})\frac{v^{n+1}_{0,0} - v^n_{0,0}}{\tau} - k(\tilde v^{n+1}_{0,0})[v^{n+1}_{0,0}]_x = \frac{\Delta x_0}{2} f_0(x_0, t_{n+1}, \tilde v^{n+1}_{0,0}) - q_0(t_{n+1}), \\ &\frac{\Delta x_1}{2}\gamma(\tilde v^{n+1}_{1,i_1})\frac{v^{n+1}_{1,i_1} - v^n_{1,i_1}}{\tau} + k(\tilde v^{n+1}_{1,i_1})[v^{n+1}_{1,i_1}]_{\bar x} = \frac{\Delta x_1}{2} f_1(x_{i_1}, t_{n+1}, \tilde v^{n+1}_{1,i_1}) + q_1(t_{n+1}). \end{aligned} \tag{16}$$

We make similar construction of the second order approximation on the border between both parts (at the point $i = i_0$). Here we need to be careful with notation and to use different indexes for differences to the left and right from the border point.

The second conjugation condition (5) can be rewritten in the following equivalent form:

$$\left.\mu k\frac{\partial w_0}{\partial x}\right|_{x=l-0}=\left.\left[k\frac{\partial w_1}{\partial x}-h_z(1-\mu)\left(w_1-\Theta\right)\right]\right|_{x=l+0},\qquad \mu=\frac{h}{H},\quad \eta=\frac{\left(H-h\right)}{H}. \tag{17}$$

Using equation (13), we approximate the left hand side flux of the equation (17) for the predictor stage as follows:

$$\mu k(v_{0,i}^n)[\tilde{v}_{0,i}^{n+1}]_{\bar{x}}+\mu\frac{\Delta x_0}{2}\left[\gamma(v_{0,i}^n)\frac{\tilde{v}_{0,i}^{n+1}-v_{0,i}^n}{\tau}-f_0(x_i,t_n,v_{0,i}^n)\right]=:J_0,\qquad i=i_0.$$

We obtain similar expression for the right hand side by formula (14):

$$k(v_{1,i}^n)[\tilde{v}_{1,i}^{n+1}]_x-\frac{\Delta x_1}{2}\left[\gamma(v_{1,i}^n)\frac{\tilde{v}_{1,i}^{n+1}-v_{1,i}^n}{\tau}-f_1(x_i,t_n,v_{1,i}^n)\right]-h_z(1-\mu)\left(\tilde{v}_{1,i}^{n+1}-\Theta\right)=:J_1.$$

Taking into account the first conjugation condition (4), i.e., continuity $v_{1,i_0}=v_{0,i_0}$, we have equality on the border:

$$J_0=J_1;$$

or the following equation for the predictor stage:

$$\begin{aligned}&\mu k(v_{0,i}^n)[\tilde{v}_{0,i}^{n+1}]_{\bar{x}}+\mu\frac{\Delta x_0}{2}\left[\gamma(v_{0,i}^n)\frac{\tilde{v}_{0,i}^{n+1}-v_{0,i}^n}{\tau}-f_0(x_i,t_n,v_{0,i}^n)\right]=\\&=k(v_{1,i}^n)[\tilde{v}_{1,i}^{n+1}]_x-\frac{\Delta x_1}{2}\left[\gamma(v_{1,i}^n)\frac{\tilde{v}_{1,i}^{n+1}-v_{1,i}^n}{\tau}-f_1(x_i,t_n,v_{1,i}^n)\right]-h_z(1-\mu)\left(\tilde{v}_{1,i}^{n+1}-\Theta\right).\end{aligned}\tag{18}$$

We have following equation for the corrector stage:

$$\begin{aligned}&\mu k(\tilde{v}_{0,i}^{n+1})[v_{0,i}^{n+1}]_{\bar{x}}+\mu\frac{\Delta x_0}{2}\left[\gamma(\tilde{v}_{0,i}^{n+1})\frac{v_{0,i}^{n+1}-v_{0,i}^n}{\tau}-f_0(x_i,t_n,\tilde{v}_{0,i}^{n+1})\right]=\\&=k(\tilde{v}_{1,i}^{n+1})[v_{1,i}^{n+1}]_x-\frac{\Delta x_1}{2}\left[\gamma(\tilde{v}_{1,i}^{n+1})\frac{v_{1,i}^{n+1}-v_{1,i}^n}{\tau}-f_1(x_i,t_n,\tilde{v}_{1,i}^{n+1})\right]-h_z(1-\mu)\left(v_{1,i}^{n+1}-\Theta\right),\\&i=i_0.\end{aligned}\tag{19}$$

The difference equations (15)-(19) together with self evident initial conditions:

$$\begin{aligned}&v_{0,i}^0=U^0(x_i),\quad 0\le i\le i_0,\\&v_{1,i}^0=U^0(x_i),\quad i_0\le i\le i_1;\end{aligned}\tag{20}$$

are complete difference scheme of the second order of approximation.